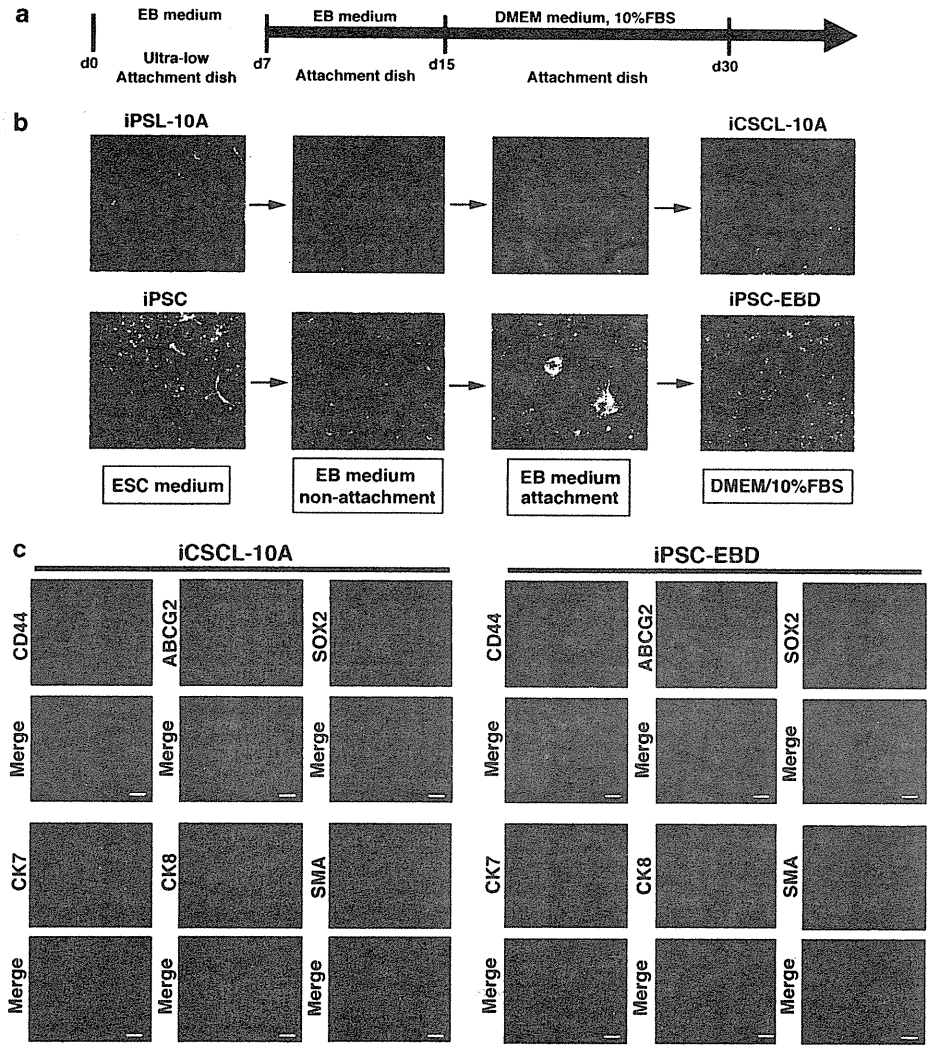

Figure 2. *In vitro* differentiation of iPSL-10A cells into induced CSCs. (**a**) Schematic representation of the *in vitro* differentiation of iPSL-10A and normal iPSCs. (**b**) Representative phase-contrast images of either iPSL-10A or normal iPSCs during embryoid body (EB)-mediated differentiation. After EBs were transferred onto gelatin-coated attachment plates and allowed to further differentiate for 8 days. These cells were then finally cultured in DMEM/10% FBS up to day 30. (**c**) Immunofluorescent analysis of lineage marker proteins in cultured iCSCL-10A and iPSC-EBD cells. Nuclei were counterstained with 4′,6-diamidino-2-phenylindole (DAPI). Scale bar, 200 μm.

Figure S3a). Furthermore, both SOX2 and CD44 expression was decreased in these cells (Supplementary Figure S3b).

A major characteristic of CSCs is their resistance to anticancer agents. We next assayed the resistance of iCSCL-10A cells to various chemotherapeutic drugs. The iCSCL-10A cells exhibited increased resistance to the established anticancer chemotherapeutic compounds, Taxol and Actinomycin D, relative to both the control MCF7 breast cancer cells and MCF-10A-Ras cells (Figure 4e). In contrast, iCSCL-10A cells were more sensitive to Salinomycin, a drug that selectively targets CSCs[6] and to the selective Pin1 inhibitor Juglone compared with MCF7 or MCF-10A-Ras cells (Figure 4e). Subsequent TUNEL (terminal deoxyribonucleotidyl transferase-mediated dUTP nick end-labeling) assay revealed that Juglone treatment selectively induces cellular apoptosis in iCSCL-10A cells as compared with parental MCF-10A cells (Figures 4f and g).

It has been shown that Pin1 function is also regulated by the phosphorylation status of both Pin1 and its target proteins.[26] Indeed, an immunoblotting analysis revealed that although Pin1 was more highly phosphorylated in iCSCL-10A cells than in iPSCs, potential Pin1-binding sites, recognized by phospho-CDK substrate antibodies, were more prominently phosphorylated in iCSCL-10A cells than in normal iPSCs (Supplementary Figure S4), suggesting a profound role of Pin1 in iCSCL-10A cells.

iCSCL-10A cells form multilineage tumors *in vivo*

We next assessed the ability of iCSCL-10A cells to form tumors in an immunosuppressed mouse model. We injected iCSCL-10A, MCF-10A-Ras, parental MCF-10A or iPSC-EBD cells subcutaneously into BALB/c nude mice and monitored them for 9 to 12 weeks. Tumors were generated using as few as 1×10^3 iCSCL-10A, which was 10-fold lower than the number of MCF-10A-Ras cells required for tumor seeding (Figure 5a). There was no evidence of tumor formation in the MCF-10A- or iPSC-EBD-injected mice up to 1×10^5 cells (Figure 5a). Histological examinations of tumor tissues revealed that iCSCL-10A cells produced a florid proliferation of small round immature cells with focal mitotic figures (Figure 5b, left). Notably, the tumor contained structures resembling differentiated cells of the bone and muscle lineages (Figure 5b, middle

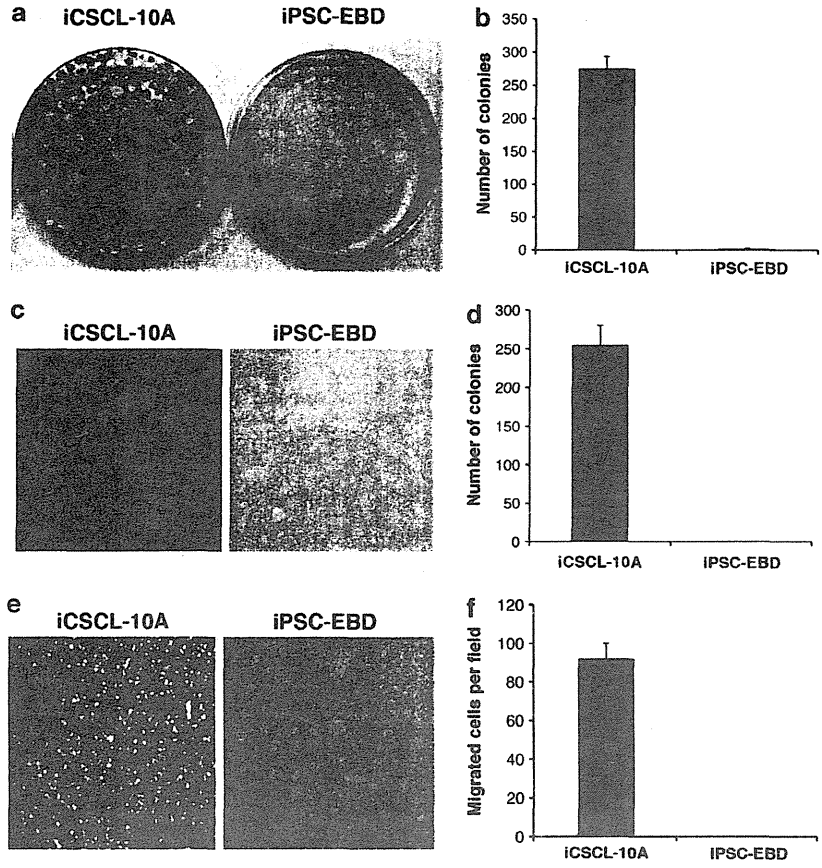

Figure 3. Malignant phenotypes of iCSCL-10A *in vitro*. (**a**, **b**) Focus formation assay of iCSCL-10A and iPSC-EBD cells. Equal numbers of cells (5×10^2) were seeded onto 10 cm plastic dishes. After 10 days, the cells were fixed and stained with crystal violet (**a**). The numbers of colonies were calculated and scored (mean ± s.d.) from three independent experiments (**b**). (**c**, **d**) iCSCL-10A and iPSC-EBD cells were plated in 0.3% soft agar and cultured for 2 weeks. Representative microscopic fields are presented (**c**). Colony formation was scored microscopically and the colony numbers (mean ± s.d.) were calculated from three independent experiments (**d**). (**e**, **f**) Cell invasion assays were performed using chemotaxis chambers in transwell tissue culture dishes as described in the Materials and methods. Representative microscopic fields are shown (**e**). Invasive cells were counted and scored in triplicate. The mean values ± s.d. were calculated from three independent experiments (**f**).

and right). Epithelial (CK), mesenchymal (vimentin), neuronal (β3-tubulin), endothelial (human CD34; does not crossreact with mouse CD34),[27] calcifying osteoblastic (osteopontin) and myoblastic (smooth muscle actin)-positive cells were detected by immunohistochemical analysis (Figure 5c). We detected, by immunofluorescence, prominent histological borders of cell populations between putatively less differentiated ($SOX2^+$/AE1/3 cytokeratin$^-$) and more differentiated cells ($SOX2^-$/AE1/3 cytokeratin$^+$) within the tumor (Figure 5d).

Cyclin-dependent kinase inhibitor p16INK4a induces cell cycle arrest and senescence in iCSCL-10A cells

The parental MCF-10A human mammary gland epithelial cells harbor a cytogenetic abnormality involving a chromosome 9 translocation resulting in the deletion of the *CDKN2A* ($p16^{INK4a}$) gene. To determine the functional role of $p16^{INK4a}$ in the proliferation and maintenance of CSC-like cells, iCSCL-10A cells were transduced with $p16^{INK4a}$ using a retrovirus vector followed by selection with puromycin. Immunoblotting analysis confirmed the stable expression of the exogenous p16 gene and decreased amounts of phosphorylated Rb (Figure 6a). Cell cycle analysis demonstrated a significantly increased G1 population of $p16^{INK4a}$-transduced cells compared with the control vector-transduced cells (Figure 6b). Cells transduced with $p16^{INK4a}$ exhibited an enlarged, flattened and irregular shape, and flow cytometric analysis revealed this effect in terms of forward scatter and side scatter profiles (Figure 6c, upper panels). These cells also positively stained with senescence-associated β-galactosidase, whereas no such cells were observed among the control vector-transduced population (Figure 6d). Concomitantly, the fraction of the CSC population that was $CD44^+/CD24^{low}$ was significantly reduced for the cells transduced with $p16^{INK4a}$ (from 86.3 to 21.0%, Figure 6c, lower panels). In line with these observations, the SOX2 localization profile was found to be significantly shifted from a nuclear to a cytoplasmic distribution, as revealed by immunofluorescence (Figure 6e).

The transduction of $p16^{INK4a}$ into iCSCL-10A cells significantly reduced the rate of tumor sphere formation down to ~20% (Figure 6f), indicating that the re-introduction of $p16^{INK4a}$ can suppress the self-renewal properties of iCSCL-10A cells. An important feature of CSCs is their increased mobility. To evaluate whether $p16^{INK4a}$ regulates cell migration in this context, wound healing assays were performed. At 6 h following cell scratching, the extent of wound closure for the empty vector control cells was 90%, whereas that for the $p16^{INK4a}$-transduced cells was significantly less, at 45% (Figure 6g).

An *in vivo* tumor-initiating assay revealed no evidence of tumor formation in the iCSCL-10A/ $p16^{INK4a}$ -injected BALB/c nude mouse (1×10^5 cells), whereas control vector-transduced

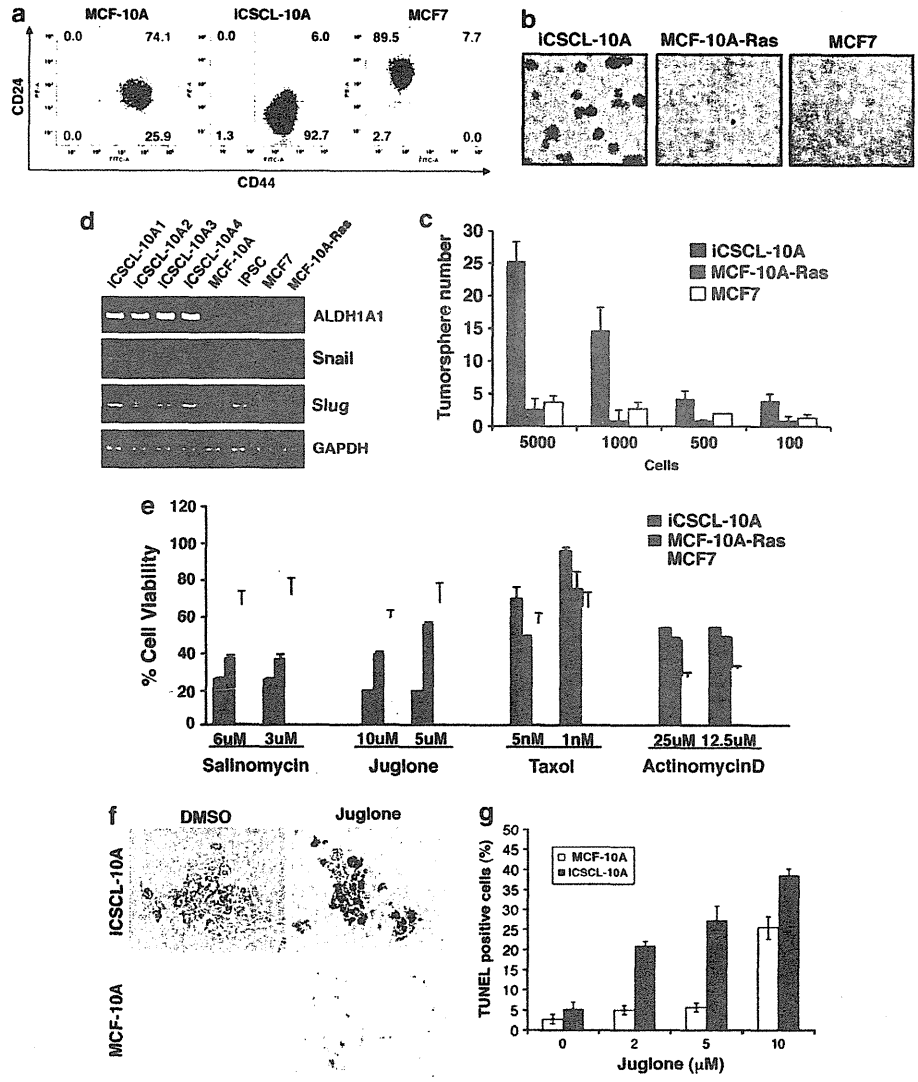

Figure 4. Characterization of the CSC properties of iCSCL-10A clones. (**a**) Flow cytometric analysis of CD44 and CD24 expression in the MCF-10A, iCSCL-10A and MCF7 cell lines. The numbers indicate the percentage of each sub-population according to the CD44/CD24 expression profile. (**b**, **c**) Tumor sphere formation assays of MCF-10A-Ras, iCSCL-10A and MCF7 cell lines. Phase-contrast images of tumor spheres are shown (**b**). Values represent the mean ± s.e.m. ($n = 3$, **c**). (**d**) Semiquantitative reverse transcriptase–PCR (RT–PCR) analysis of the expression of CSC- or epithelial-to-mesenchymal transition (EMT)-related genes. Glyceraldehyde-3-phosphate dehydrogenase (GAPDH) was analyzed as a control. (**e**) Viability of MCF-10A-Ras, iCSCL-10A and MCF7 cell lines treated with various chemotherapeutic agents for 72 h by MTT assay. Values represent the mean ± s.e.m. ($n = 3$). (**f**, **g**) iCSCL-10A and parental MCF-10A cells were treated with Juglone (5 μm) for 24 h and subjected to TUNEL (terminal deoxyribonucleotidyl transferase-mediated dUTP nick end-labeling) assay (**f**, brown color). TUNEL-positive cells were scored from triplicate independent experiments (**g**). Values represent the mean ± s.e.m. ($n = 3$).

iCSCL-10A cells still formed tumors, indicating that iCSCL-10A cells had lost their tumor-initiating properties following the re-expression of $p16^{INK4a}$ (Supplementary Figure S5). Taken together, these results together indicate that the re-introduction of $p16^{INK4a}$ can indeed attenuate the CSC properties of iCSCL-10A cells.

DISCUSSION

We have demonstrated in the current study that the introduction of defined reprogramming factors and subsequent partial cell differentiation generate cells with a tumorigenic phenotype and CSC-like properties from nontransformed human MCF-10A mammary epithelial cells. These cells show a resistance profile against anticancer agents that is normally associated with CSCs. Moreover, these transformed cells can be maintained in culture in Dulbecco's modified Eagle's medium (DMEM) supplemented with 10% fetal bovine serum (FBS), permitting easy manipulation and amenability to large-scale drug screening and could therefore provide a valuable basis for the further analysis of CSC characteristics and drug development strategies designed to target CSCs.

Several studies have suggested that the molecular circuitry controlling pluripotency in stem cells is also important for the tumor-initiating ability of cancer cells. In fact, the pluripotent cell markers OCT4, SOX2, Klf4 and Nanog have been shown to be expressed in certain cancer cell types and to play important roles in oncogenesis.[28–31] A recent study has reported a crucial role for SOX2 but not OCT4 and Nanog in breast CSCs. SOX2 expression was found in this report to be induced upon the formation of

a

Tumor seeding				
Cell injected	iCSCL-10A	MCF-10A-Ras	MCF-10A	iPSC-EBD
$1X10^5$	12/12	4/12	0/12	0/12
$1X10^4$	12/12	3/12	ND	ND
$1X10^3$	12/12	0/12	ND	ND

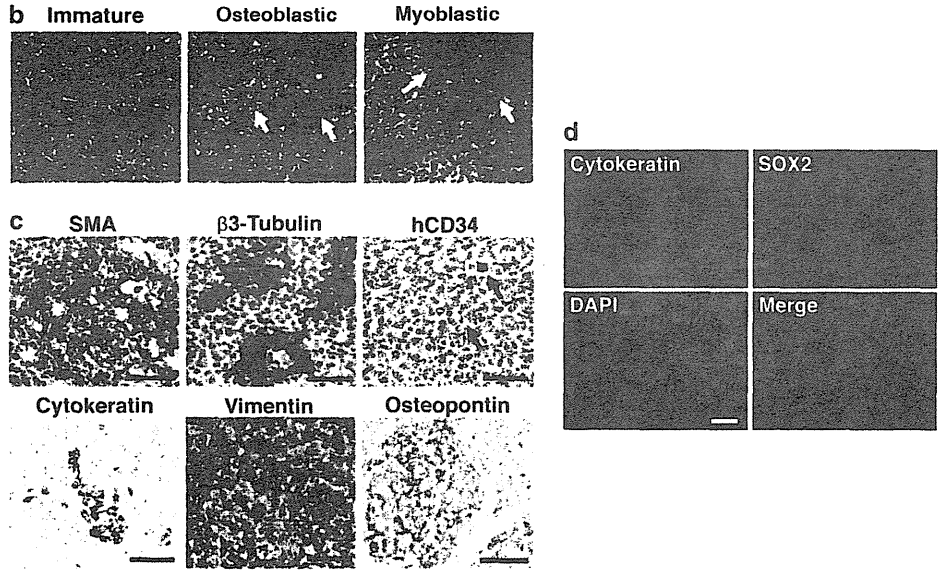

Figure 5. iCSCL-10A cells form hierarchically organized tumors *in vivo*. (**a**) Tumor-seeding ability of iCSCL-10A, MCF-10A-Ras parental MCF-10A cells and iPSC-EBD. The indicated numbers of each cell type were injected into immunocompromised mice. The tumor-initiation ability per injection was then monitored. (**b**) Hematoxylin and eosin (H&E) staining of primary tumor tissues. Scale bar, 500 μm. (**c**) Immunohistochemical analysis of primary tumor tissues derived from iCSCL-10A cells using antibodies targeting hCD34 (endothelial), smooth muscle actin (SMA; myoblastic), β3-tubulin (neural), cytokeratin (CAM5.2, epithelial), vimentin (mesenchymal) and osteopontin (osteoblastic). Scale bar, 500 μm. (**d**) Immunofluorescent analysis with antibodies targeting SOX2 and cytokeratin (AE1/AE3). Nuclei were counterstained with 4′,6-diamidino-2-phenylindole (DAPI). Scale bar, 500 μm.

tumor spheres from natural breast tumor cultures and breast carcinoma cell lines.[32] SOX2 has been shown to be expressed in a variety of early stage of breast carcinomas and metastatic lymph nodes.[33] Hence, high SOX2 expression in iCSCL-10A cells may contribute to the high tumor-initiating ability of these cells.

The current picture of carcinogenesis from iPSCs is ambiguous. Pre-iPS cells have been defined as incompletely reprogrammed multipotent stem cells that arise during the induction of iPSCs.[13,34] Like iPSCs, pre-iPS cells have been shown to form tumors in immunosuppressed mouse models, but their histology is not considered to be that of a teratoma[13] but rather a phenotype that is reminiscent of the induced CSCs described herein. Furthermore, iPS reprogramming of p53 knockout or p53 mutant mouse embryonic fibroblasts led to the development of cells with a potential to form malignant tumors with sarcoma-like morphology in nude mice.[35] Moreover, mouse iPSCs cultured in mouse Lewis lung carcinoma conditioned medium acquire the characteristics of CSCs.[36] These data suggest that iPS reprogramming factors might be adequate to transform somatic cells with certain genetic defects or specific culture conditions. However, the iPS-mediated malignant cells analyzed to date come from a rodent source, cells that are believed to be more susceptible to transformation than human cells.[37] Meanwhile, the current system using nontumorigenic human mammary epithelial MCF-10A cells may cast new light on the susceptibility of nontumorigenic human mammary epithelial cells to neoplastic reprogramming. How similar the CSC-like cells described in the current paper are to human pre-iPS remains unknown. However, such a comparison may be an important point of departure for future studies concerned with both CSCs and the oncogenic potential of cells produced using iPS technology.

MCF-10A is an immortalized but nontransformed human breast epithelial cell line that is widely used in molecular studies of cancer.[19] In addition, although these cells have only a small number of chromosome translocations, one of which results in the depletion of the *p16INK4a* gene,[18] they show a normal mammary epithelial cell morphology and phenotype and can successfully form mammary acini in 3D matrigel cultures.[20] These characteristics of MCF-10A cells prompted us to use them for our current model system. As many previous studies have already reported, the INK4A gene locus is completely silenced and $p16^{INK4a}$ is not usually expressed in pluripotent stem cells such as ESCs and iPSCs.[38,39] Indeed, several different groups have demonstrated that the INK4A gene locus critically impairs successful reprogramming to pluripotent stem cells and that it represents a principal barrier to iPS cell reprogramming through the induction of reprogramming-induced senescence.[40–42] In human somatic cells, the inhibition of $p16^{INK4a}$ enhances the iPSC generation, increasing both the kinetics of reprogramming and the number of emerging iPSC colonies.[39] Furthermore, our current study demonstrates that the re-expression of $p16^{INK4a}$ can indeed attenuate the CSC properties and *in vivo* tumorigenicity of iCSCL-10A cells. Thus, the loss of $p16^{INK4a}$ may affect not only the oncogenic reprogramming but also the maintenance of malignant properties of iCSC-10A cells.

In general, CSCs have increased resistance to conventional anticancer chemotherapeutic agents.[5] We observed that iCSCL-10A cells exhibited higher sensitivity to the Pin1-selective inhibitor

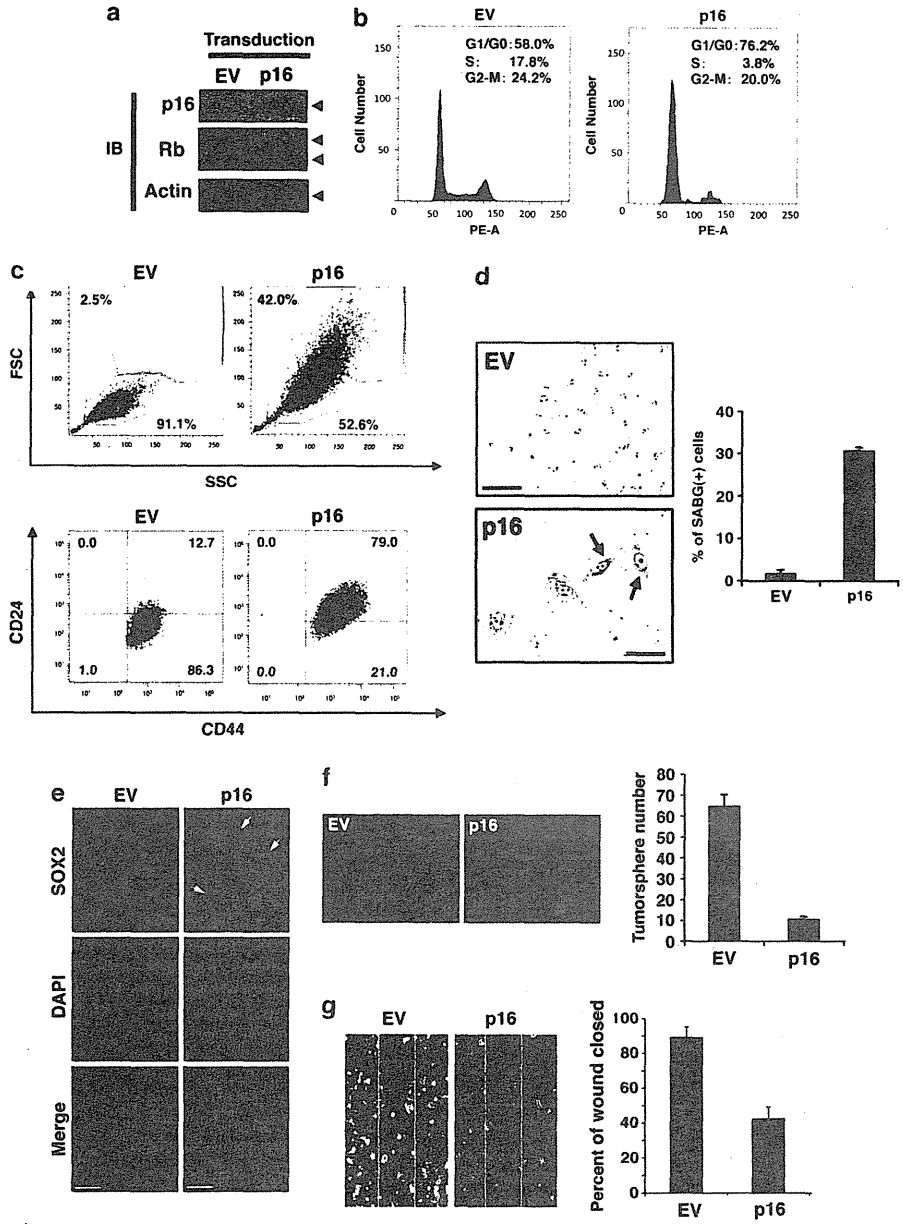

Figure 6. Cyclin-dependent kinase inhibitor p16 suppresses the CSC properties of iCSCL-10A cells and induces cellular senescence. (**a**) Immunoblotting analysis of p16 and Rb in iCSCL-10A cells transduced with the p16 vector or with an empty vector (EV) control retrovirus. Actin was used as a loading control. (**b**) Flow cytometric analysis of the cell cycle status following propidium iodide (PI) staining of iCSCL-10A cells transduced with p16 or EV. (**c**) Flow cytometric analysis of forward scatter (FSC) versus side scatter (SSC) dot plot (upper panels) and CD44/CD24 expression (lower panels). Note that p16 transduction results in the appearance of large-sized cells. (**d**) p16-transduced iCSCL-10A cells were subjected to senescence-associated β-galactosidase staining (SABG). Phase-contrast images of the cells are shown. Arrows indicate positive signals shown in blue (photomicrographs). Scale bar, 200 μm. Bars indicate the percentage of SABG-positive cells for each cell species (histogram). Values represent the mean ± s.e.m. ($n = 3$). (**e**) Re-expression of p16 promotes SOX2 translocation from the nucleus to the cytoplasm. Immunofluorescent analysis of SOX2 in p16-transduced iCSCL-10A cells. Arrows indicate cytoplasmic localization of SOX2. Nuclei were counterstained with 4′,6-diamidino-2-phenylindole (DAPI). (**f**) p16 transduction abrogates the tumor sphere-forming ability of iCSCL-10A cells. Phase-contrast images of tumor spheres transduced with p16 or EV and quantification of tumor sphere formation. Values represent the means ± s.e.m. ($n = 3$). (**g**) Effects of p16 on wound healing. Confluent monolayers of the iCSCL-10A cells transduced with either p16 or EV were mechanically wounded using the tip of a pipette. After 6 h, the cells were fixed and images were captured. Wound closures were scored using ImageJ software. Values represent the mean ± s.e.m. ($n = 3$).

Juglone compared with MCF7 or MCF-10A-Ras cells, which may reflect the importance of Pin1 in the maintenance of pluripotency of CSC through the binding and stabilization of key 'stemness' factors such as Nanog and OCT4 as is the case for human iPSCs and murine ESCs.[21,43] This drug-sensitivity profile, together with our finding that Pin1 expression is induced during the nuclear reprogramming process, tempts us to propose that iCSCL-10A cells are distinct from the parental MCF-10A cells as well as from various transformed cancer cell lines with respect to the dependency on Pin1. Considered along with our current results,

this leads us to speculate that Pin1 could be an essential factor for the self-renewal and proliferation of CSC, and even perhaps a potential molecular target for CSC-based therapy.

In summary, we here describe the oncogenic transformation of mammary epithelial cells and consequent generation of a potentially valuable model system for the study of CSCs and development of alternative anticancer strategies that target CSCs.

MATERIALS AND METHODS

Cell culture

MCF-10A and MCF7 cells were obtained from American Type Culture Collection (ATCC, Manassas, VA, USA). MCF-10A cells cultured in mammary epithelial cell growth medium (MEGM; Sanko Junyaku, Tokyo, Japan). Human primary mammary epithelial cells were purchased from Kurabo Industrial (Osaka, Japan). Human iPSCs and iPSLCs were cultured in hESC culture medium (KNOCKOUT DMEM; Invitrogen, San Diego, CA, USA) supplemented with 20% KNOCKOUT SR (Invitrogen), 1% GlutaMAX (Invitrogen), 100 μM nonessential amino acids (Invitrogen), 1% penicillin/streptomycin, 50 μM β-mercaptoethanol and 10 ng/ml basic fibroblast growth factor. iCSCL-10A and MEFs were cultured in DMEM supplemented with 10% FBS and 1% penicillin/streptomycin.

Cell reprogramming and transformation

MCF-10A cells were transduced with retroviral vectors encoding nuclear reprogramming factors as described previously.[44] Briefly, the retroviral vector plasmids pMXs-hOCT4, pMXs-hSOX2, pMXs-hKlf4, pMXs-hc-Myc (Addgene, Cambridge, MA, USA) and VSV-G were introduced into Plat-E cells using Effectene transfection reagent (QIAGEN, Maryland, MD, USA). After 48 h, virus-containing supernatants were passed through a 0.45 μm filter and supplemented with 10 μg/ml polybrene. MCF-10A cells were seeded at 6×10^5 cells per 100 mm dish 24 h before incubation in the virus/polybrene-containing supernatants for 16 h. Cells were then washed and returned to fresh MEGM medium. After 6 days, the cells were plated on irradiated MEFs and the MEGM culture medium was replaced with hESC culture medium 24 h later. Cells were maintained at 37 °C in a 5% CO_2 incubator for 21 days.

Alkaline phosphatase staining

Alkaline phosphatase staining was performed using the Leukocyte Alkaline Phosphatase kit (Sigma-Aldrich, St Louis, MO, USA) according to the manufacturer's protocol.

EB formation and spontaneous differentiation

The iPSL-10A cells were dissociated using accutase and seeded on a Matrigel (BD Biosciences, San Diego, CA, USA) coated dish in MEF-conditioned hESC medium for feeder-free culture. The iPSL-10A cells were also dissociated using accutase and plated on ultra low-attachment plates (Cell Seed) at a density of 1×10^4 cells per 6 wells in differentiation medium (KNOCKOUT DMEM supplemented with 20% FBS, 1% GlutaMAX; Invitrogen), 100 μM nonessential amino acids (Invitrogen), 1% penicillin/streptomycin and 50 μM β-mercaptoethanol. After 7 days, the embryoid body-like colonies were transferred to 0.1% gelatin-coated culture dishes and cultured for a further 8 days in the same medium. Finally, medium was replaced by DMEM supplemented with 10% FBS for 15 days before fixation and staining.

In vivo tumor formation assay

Cells were washed twice with antibiotic-free and serum-free cell culture medium and finally resuspended in 0.1 ml of serum-free culture medium. The cell suspension was then mixed with an equal volume of Matrigel (BD Biosciences) and injected subcutaneously into 6-week-old irradiated (4 Gy) BALB/c nude mice (CLEA, Tokyo, Japan). Injections were performed 1 day after irradiation. Tumors were surgically removed 9 to 12 weeks later. Representative tumor tissues were fixed in 3% formalin, embedded in paraffin wax and sectioned at a thickness of 10 μm. Sections were stained with hematoxylin and eosin for pathological examination, or processed for immunohistochemical analysis. All animal protocols were approved by the institutional Administrative Panel on Laboratory Animal Care of Yokohama City University.

RNA isolation and reverse transcriptase–PCR

Total RNA was extracted using TRIzol (Invitrogen). Complementary DNA synthesis was performed with ReverTraAce-α (Toyobo, Osaka, Japan) in accordance with the manufacturer's instructions. PCR was performed with ExTaq (Takara Bio, Shiga, Japan) using the following primers: human SOX2 (endogenous) fwd 5′-GGGAAATGGGAGGGGTGCAAAAGAGG-3′, rev 5′-TTGCGTGAGTGTGGATGGGATTGGTG-3′; human OCT4 (endogenous) fwd 5′-GACAGGGGGAGGGGAGGAGCTAGG-3′, rev 5′-CTTCCCTCCAACCA GTTGCCCCAAAC-3′; human Nanog fwd 5′-CAGCCCtGATTCTTCCACCAGT CCC-3′, rev 5′-tGGAAGgTTCCCAGTCGGGTTCACC-3′; human DNMT3B fwd 5′-TGCTGCTCACAGGGCCCGATACTTC-3′, rev 5′-TCCTTTCGAGCTCAGTGCA CCACAAAAC-3′; human UTF1 fwd 5′-CCGTCGCTGAACACCGCCCTGCTG-3′, rev 5′-CGCGCTGCCCAGAATGAAGCCCAC-3′; human GAPDH fwd 5′-GTGG ACCTGACCTGCCGTCT-3′, rev 5′-GGAGGAGTGGGTGTCGCTGT-3′; human Snail fwd 5′-TCAAGATGCACATCCGAAGC-3′, rev 5′-AGGACACAGAACCAG AAAATGG-3′; Slug fwd 5′-CAGACCCTGGTTGCTTCAAG-3′, rev 5′-CACAGGAG AAAATGCCTTTGG-3′; human ALDH1A1 fwd 5′-TAAGCATCTCCTTACAGTC AC-3′, rev 5′-TGTTAAGTACTTCAAGAGTCAC-3′.

Immunohistochemistry and immunocytochemistry

For immuncytochemistry, cells were fixed with 4% paraformaldehyde for 15 min at 4 °C, washed with phosphate-buffered saline and then permeabilized using 0.1% Triton X-100 and blocked with 5% goat serum in 0.1% bovine serum albumin. Primary antibodies were diluted in 0.1% bovine serum albumin and incubated with the fixed cells for 1 h at room temperature. For immunohistochemistry, paraffin-embedded tissue sections were subjected to antigen retrieval with microwave irradiation in citrate buffer (pH 6.0). This was followed by incubation with primary antibody at room temperature for 60 min. After incubation with secondary antibody at room temperature for 60 min, the sections were stained with VECTASTAIN Universal Elite ABC Kit (Vector Laboratories, Burlingame, CA, USA) according to the manufacturer's instructions. The primary antibodies used in this study were as follows: anti-OCT4 (1:300; Santa Cruz Biotechnology, Santa Cruz, CA, USA), anti-SOX2 (1:300; Millipore, Billerrica, MA, USA), anti-TRA-1-60 (1:200; eBioscience, San Diego, CA, USA), anti-Nanog (1:300; ReproCELL, Yokohama, Japan), anti-Cytokeratin 7 (1:50, M7018; Dako Cytomation, Düsseldorf, Germany), anti-Cytokeratin 8 (1:50; Becton Dickinson, Mountain view, CA, USA), anti-cytokeratin AE1/AE3 (1:500; Abcam, Cambridge, MA, USA), anti-CD44 (1:100; Cell Signaling. Danvers, MA, USA), anti-ABCG2 (1:100; BioLegend, San Diego, CA, USA), anti-β-Tubulin III (1:100; Sigma), anti-hCD34 (1:100; Abcam), anti-Osteopontin (1:100; Sigma), anti-Vimentin (V9, 1:300; Abcam) and anti-smooth muscle actin (1:100; Sigma).

Cell invasion assay

Cell invasion assay was performed in 24-well format Transwell inserts (8 μm pore, BD Biosciences) coated with 1 mg/ml matrigel (BD Biosciences) as described previously.[45] Invasive cells were counted and scored in triplicate (lower chamber).

Soft agar colony formation assay

Soft agar colony formation assays were performed by seeding 5×10^3 cells in 60-mm tissue culture dishes containing 0.3% top low-melting point agarose/0.5% bottom low-melting point agarose. Cells were fed every 4 days and colonies were counted and measured after 2 weeks.

Karyotyping

Karyotyping was performed by Nihon Gene Research Laboratories (Sendai, Japan), as described previously.[44] At least 15 metaphase spreads per genotype and from at least two independent cultures per genotype were scored for chromosomal aberrations.

Tumor sphere formation assay

Single cells were seeded in ultra low-attachment dishes (Corning, New York, NY, USA) at a density of 2×10^4 cells/ml and cultured for 7 days in serum-free DMEM/Ham's F12 nutrient mixture (1:1, v/v) supplemented with 5 mg/ml insulin, 0.5 mg/ml hydrocortisone, 2% B27 and 20 ng/ml epidermal growth factor.

Wound healing assay

Cell layers were gently wounded through the central axis of the plate using a pipette tip. The migration of cells into the wound was observed at 6 h in six random selected microscopic fields. Wound closures were quantified using an image processing and analysis software program (ImageJ 1.40g, Bethesda, MD, USA).

CONFLICT OF INTEREST

The authors declare no conflict of interest.

ACKNOWLEDGEMENTS

We thank A Kondo, T Taniguchi, Y Kojima, Y Watanabe, M Tanaka and N Sakurai for technical assistance and discussion. This work was in part supported by Grant-in-Aid for Scientific Research on Innovative Areas and the Japan Health Sciences Foundation, and grants from the Uehara Memorial Foundation and Takeda Science Foundation to AR.

REFERENCES

1 Visvader JE, Lindeman GJ. Cancer stem cells in solid tumours: accumulating evidence and unresolved questions. *Nat Rev Cancer* 2008; **8**: 755–768.
2 Al-Hajj M, Wicha MS, Benito-Hernandez A, Morrison SJ, Clarke MF. Prospective identification of tumorigenic breast cancer cells. *Proc Natl Acad Sci USA* 2003; **100**: 3983–3988.
3 Singh SK, Clarke ID, Terasaki M, Bonn VE, Hawkins C, Squire J *et al.* Identification of a cancer stem cell in human brain tumors. *Cancer Res* 2003; **63**: 5821–5828.
4 Clevers H. The cancer stem cell: premises, promises and challenges. *Nat Med* 2011; **17**: 313–319.
5 Dean M, Fojo T, Bates S. Tumour stem cells and drug resistance. *Nat Rev Cancer* 2005; **5**: 275–284.
6 Gupta PB, Onder TT, Jiang G, Tao K, Kuperwasser C, Weinberg RA *et al.* Identification of selective inhibitors of cancer stem cells by high-throughput screening. *Cell* 2009; **138**: 645–659.
7 Dick JE. Looking ahead in cancer stem cell research. *Nat Biotechnol* 2009; **27**: 44–46.
8 Berry PA, Maitland NJ, Collins AT. Androgen receptor signalling in prostate: effects of stromal factors on normal and cancer stem cells. *Mol Cell Endocrinol* 2008; **288**: 30–37.
9 Dey D, Saxena M, Paranjape AN, Krishnan V, Giraddi R, Kumar MV *et al.* Phenotypic and functional characterization of human mammary stem/progenitor cells in long term culture. *PLoS One* 2009; **4**: e5329.
10 Rosen JM, Jordan CT. The increasing complexity of the cancer stem cell paradigm. *Science* 2009; **324**: 1670–1673.
11 Lessard J, Sauvageau G. Bmi-1 determines the proliferative capacity of normal and leukaemic stem cells. *Nature* 2003; **423**: 255–260.
12 Werbowetski-Ogilvie TE, Bosse M, Stewart M, Schnerch A, Ramos-Mejia V, Rouleau A *et al.* Characterization of human embryonic stem cells with features of neoplastic progression. *Nat Biotechnol* 2009; **27**: 91–97.
13 Takahashi K, Yamanaka S. Induction of pluripotent stem cells from mouse embryonic and adult fibroblast cultures by defined factors. *Cell* 2006; **126**: 663–676.
14 Yu J, Vodyanik MA, Smuga-Otto K, Antosiewicz-Bourget J, Frane JL, Tian S *et al.* Induced pluripotent stem cell lines derived from human somatic cells. *Science* 2007; **318**: 1917–1920.
15 Miyoshi N, Ishii H, Nagai K, Hoshino H, Mimori K, Tanaka F *et al.* Defined factors induce reprogramming of gastrointestinal cancer cells. *Proc Natl Acad Sci USA* 2010; **107**: 40–45.
16 Carette JE, Pruszak J, Varadarajan M, Blomen VA, Gokhale S, Camargo FD *et al.* Generation of iPSCs from cultured human malignant cells. *Blood* 2010; **115**: 4039–4042.
17 Utikal J, Maherali N, Kulalert W, Hochedlinger K. Sox2 is dispensable for the reprogramming of melanocytes and melanoma cells into induced pluripotent stem cells. *J Cell Sci* 2009; **122**(Pt 19): 3502–3510.
18 Cowell JK, LaDuca J, Rossi MR, Burkhardt T, Nowak NJ, Matsui S. Molecular characterization of the t(3;9) associated with immortalization in the MCF10A cell line. *Cancer Genet Cytogenet* 2005; **163**: 23–29.
19 Soule HD, Maloney TM, Wolman SR, Peterson Jr. WD, Brenz R, McGrath CM *et al.* Isolation and characterization of a spontaneously immortalized human breast epithelial cell line, MCF-10. *Cancer Res* 1990; **50**: 6075–6086.
20 Debnath J, Muthuswamy SK, Brugge JS. Morphogenesis and oncogenesis of MCF-10A mammary epithelial acini grown in three-dimensional basement membrane cultures. *Methods* 2003; **30**: 256–268.
21 Nishi M, Akutsu H, Masui S, Kondo A, Nagashima Y, Kimura H *et al.* A distinct role for Pin1 in the induction and maintenance of pluripotency. *J Biol Chem* 2011; **286**: 11593–11603.
22 Desbaillets I, Ziegler U, Groscurth P, Gassmann M. Embryoid bodies: an in vitro model of mouse embryogenesis. *Exp Physiol* 2000; **85**: 645–651.
23 Liu M, Casimiro MC, Wang C, Shirley LA, Jiao X, Katiyar S *et al.* p21CIP1 attenuates Ras- and c-Myc-dependent breast tumor epithelial mesenchymal transition and cancer stem cell-like gene expression in vivo. *Proc Natl Acad Sci USA* 2009; **106**: 19035–19039.
24 Ginestier C, Hur MH, Charafe-Jauffret E, Monville F, Dutcher J, Brown M *et al.* ALDH1 is a marker of normal and malignant human mammary stem cells and a predictor of poor clinical outcome. *Cell Stem Cell* 2007; **1**: 555–567.
25 Bhat-Nakshatri P, Appaiah H, Ballas C, Pick-Franke P, Goulet Jr R, Badve S *et al.* SLUG/SNAI2 and tumor necrosis factor generate breast cells with CD44+/CD24- phenotype. *BMC Cancer* 2010; **10**: 411.
26 Lu PJ, Zhou XZ, Liou YC, Noel JP, Lu KP. Critical role of WW domain phosphorylation in regulating phosphoserine binding activity and Pin1 function. *J Biol Chem* 2002; **277**: 2381–2384.
27 Scaffidi P, Misteli T. In vitro generation of human cells with cancer stem cell properties. *Nat Cell Biol* 2011; **13**: 1051–1061.
28 Hochedlinger K, Yamada Y, Beard C, Jaenisch R. Ectopic expression of Oct-4 blocks progenitor-cell differentiation and causes dysplasia in epithelial tissues. *Cell* 2005; **121**: 465–477.
29 Chen Y, Shi L, Zhang L, Li R, Liang J, Yu W *et al.* The molecular mechanism governing the oncogenic potential of SOX2 in breast cancer. *J Biol Chem* 2008; **283**: 17969–17978.
30 Wei D, Kanai M, Huang S, Xie K. Emerging role of KLF4 in human gastrointestinal cancer. *Carcinogenesis* 2006; **27**: 23–31.
31 Clark AT. The stem cell identity of testicular cancer. *Stem Cell Rev* 2007; **3**: 49–59.
32 Leis O, Eguiara A, Lopez-Arribillaga E, Alberdi MJ, Hernandez-Garcia S, Elorriaga K *et al.* Sox2 expression in breast tumours and activation in breast cancer stem cells. *Oncogene* 2012; **31**: 1354–1365.
33 Lengerke C, Fehm T, Kurth R, Neubauer H, Scheble V, Muller F *et al.* Expression of the embryonic stem cell marker SOX2 in early-stage breast carcinoma. *BMC Cancer* 2011; **11**: 42.
34 Silva J, Barrandon O, Nichols J, Kawaguchi J, Theunissen TW, Smith A. Promotion of reprogramming to ground state pluripotency by signal inhibition. *PLoS Biol* 2008; **6**: e253.
35 Sarig R, Rivlin N, Brosh R, Bornstein C, Kamer I, Ezra O *et al.* Mutant p53 facilitates somatic cell reprogramming and augments the malignant potential of reprogrammed cells. *J Exp Med* 2010; **207**: 2127–2140.
36 Chen L, Kasai T, Li Y, Sugii Y, Jin G, Okada M *et al.* A model of cancer stem cells derived from mouse induced pluripotent stem cells. *PLoS One* 2012; **7**: e33544.
37 Hahn WC, Counter CM, Lundberg AS, Beijersbergen RL, Brooks MW, Weinberg RA. Creation of human tumour cells with defined genetic elements. *Nature* 1999; **400**: 464–468.
38 Ohm JE, McGarvey KM, Yu X, Cheng L, Schuebel KE, Cope L *et al.* A stem cell-like chromatin pattern may predispose tumor suppressor genes to DNA hypermethylation and heritable silencing. *Nat Genet* 2007; **39**: 237–242.
39 Li H, Collado M, Villasante A, Strati K, Ortega S, Canamero M *et al.* The Ink4/Arf locus is a barrier for iPS cell reprogramming. *Nature* 2009; **460**: 1136–1139.
40 Utikal J, Polo JM, Stadtfeld M, Maherali N, Kulalert W, Walsh RM *et al.* Immortalization eliminates a roadblock during cellular reprogramming into iPS cells. *Nature* 2009; **460**: 1145–1148.
41 Marion RM, Strati K, Li H, Murga M, Blanco R, Ortega S *et al.* A p53-mediated DNA damage response limits reprogramming to ensure iPS cell genomic integrity. *Nature* 2009; **460**: 1149–1153.
42 Banito A, Rashid ST, Acosta JC, Li S, Pereira CF, Geti I *et al.* Senescence impairs successful reprogramming to pluripotent stem cells. *Genes Dev* 2009; **23**: 2134–2139.
43 Moretto-Zita M, Jin H, Shen Z, Zhao T, Briggs SP, Xu Y. Phosphorylation stabilizes Nanog by promoting its interaction with Pin1. *Proc Natl Acad Sci USA* 2010; **107**: 13312–13317.
44 Takahashi K, Tanabe K, Ohnuki M, Narita M, Ichisaka T, Tomoda K *et al.* Induction of pluripotent stem cells from adult human fibroblasts by defined factors. *Cell* 2007; **131**: 861–872.
45 Ryo A, Uemura H, Ishiguro H, Saitoh T, Yamaguchi A, Perrem K *et al.* Stable suppression of tumorigenicity by Pin1-targeted RNA interference in prostate cancer. *Clin Cancer Res* 2005; **11**: 7523–7531.

Supplementary Information accompanies the paper on the Oncogene website (http://www.nature.com/onc)

Jpn. J. Infect. Dis., 66, 76-78, 2013

Laboratory and Epidemiology Communications

An Outbreak of Parainfluenza Virus Type 4 Infections among Children with Acute Respiratory Infections during the 2011-2012 Winter Season in Yamagata, Japan

Chieko Abiko[1], Katsumi Mizuta[1]*, Yoko Aoki[1], Tatsuya Ikeda[1], Tsutomu Itagaki[2], Masahiro Noda[3], Hirokazu Kimura[3], and Tadayuki Ahiko[1]

[1]*Department of Microbiology, Yamagata Prefectural Institute of Public Health, Yamagata 990-0031;*
[2]*Yamanobe Pediatric Clinic, Yamagata 990-0301; and*
[3]*Infectious Disease Surveillance Center, National Institute of Infectious Diseases, Tokyo 208-0011, Japan*

Communicated by Makoto Takeda

(Accepted November 8, 2012)

Human parainfluenza virus type 4 (HPIV4) belongs to genus *Rubulavirus*, subfamily *Paramyxovirinae* of family *Paramyxoviridae* (1). Although serological surveys indicate that infection may be common, and even universal, reports and descriptions of HPIV4-associated diseases are limited (1-4). Thus, although mild and severe respiratory illness associated with HPIV4 infections are reported, correlations between HPIV4 infections and specific clinical syndromes, age of the child, and time of the year, or seasonal patterns have not been established thus far (1-8). Due to the difficulties in isolating HPIV4, such as slow growth, trypsin concentration, and subtle cytopathic effect (4), its diagnosis has probably been underestimated in the past. However, even though previously undetected cases can now be identified with more sensitive methods such as real-time reverse transcription-PCR (RT-PCR) (1,2), the number of HPIV4 infections reported is still quite low. For example, only 88 cases, including our 28 cases from Yamagata in 2011, were reported between 1982 and 2011 in Japan, according to the National Epidemiological Surveillance of Infectious Diseases (NESID) system (9). In this study, we describe an outbreak of HPIV4 infections during the 2011-2012 winter season in Yamagata, Japan.

We carried out a longitudinal epidemiological study of acute respiratory infections (ARIs) among children in Yamagata, Japan, primarily based on virus isolation using a microplate method (10). Six cell lines, namely HEF, HEp-2, Vero or VeroE6, MDCK, RD-18S, and GMK, have been used since 2001. In 2008, we added the HMV-II cell line, primarily for the isolation of HPIVs (10-12). Then, when we accidentally succeeded in isolating one HPIV4 strain from a nasopharyngeal sample collected in October 2011, we added the LLC-MK2 cell line, which is reportedly sensitive for the isolation of HPIV4 (13). Further, we performed RT-PCR screening for HPIV4 in fresh and stocked frozen samples. In the latter effort, cases found to be positive using the influenza virus test kit were excluded. Finally, we included 1,499 nasopharyngeal swab specimens obtained from patients with ARIs at pediatric clinics between January

Table 1. Primers used to amplify and sequence the HN region to differentiate between HPIV4a and HPIV4b

Primer	Sequence (5′-3′)	Position (AB543336)
Para4-HN-F1-710	CAACAATCCAGARRGACGTCACA	7409-7431
Para4-HN-F2-711	AGATTAYCCCAATTTTATTCCAACTG	7995-8220
Para4-HN-F3-712	AGGAGCAAAAGAYTCATACACAATAACT	8583-8610
Para4-HN-R2-715	CATTCTTTTGGRCAAGCCTTA	8930-8910
Para4-HN-R3-717	GGTTCCGCTTGATGGACTGT	9508-9489
Para4-HN-R4-718	GGCCGATGGTCCTTCGTATA	9567-9548
Para4-HN-F4-719	CCATCATTYTCCYTARGTCAAA	8049-8071
Para4-HN-F5-720	TGCAGAGGGTCGMYTATATAAYATTG	8721-8746
Para4-HN-R3-721	CGATTCYTCCCRTCATTTAAAT	8228-8207
Para4-HN-R5-723	TGATTCTATADAGGCTYGGATADGG	8812-8788
		Position (AB543337)
Para4-HN-R1-714	TTTGTTATTGATGGGTGATGTTTCAC	9467-9443

*Corresponding author: Mailing address: Department of Microbiology, Yamagata Prefectural Institute of Public Health, Tokamachi 1-6-6, Yamagata 990-0031, Japan. Tel: +81-23-627-1373, Fax: +81-23-641-7486, E-mail: mizutak@pref.yamagata.jp

2011 and April 2012. We screened the polymerase L gene coding region using the previously reported AVU-RUB-F1, AVU-RUB-F2, and AVU-RUB-R primers (14), and we further amplified the hemagglutinin-neuraminidase (HN) glycoprotein region in HPIV4-positive specimens to differentiate between HPIV4a and HPIV4b using our original primers shown in Table 1. We registered sequence data with GenBank (accession nos. AB753462-AB753479). When we found syncytia formation on the HMV-II and/or LLC-MK2 cell lines, we also carried out immunofluorescent staining to identify HPIV4, using two commercially available antibodies: mouse anti-parainfluenza 4 MAB8780 (Millipore, Temecula, Calif., USA) and FITC-conjugated rabbit anti-mouse immunoglobulins (DAKO, Glostrup, Denmark).

Among the 1,499 clinical specimens, all 43 HPIV4-positive cases were detected by RT-PCR, and the virus was isolated on the HMV-II and/or LLC-MK2 cell lines in 12 of the 43 cases (Fig. 1). The monthly distribution of HPIV4 detection during the study period is shown in Fig. 2. Further, 37 (86%) HPIV4-positive cases were found between September 2011 and February 2012. In other months, only 0-1 cases were detected. Sequence data were analyzed with CLUSTAL W version 1.83, and a phylogenetic tree was constructed via the neighbor-joining method (Fig. 3). Among the 43 HPIV4-positive cases, 7 were identified as HPIV4a, 11 as HPIV4b, while the others remained unidentified because the HN region was not amplified enough for the analysis.

Among the 43 HPIV4-positive cases, 4 patients (9.3%) were aged <1 years, 10 (23.2%) were aged 1 year, 2 (4.7%) were aged 2 years, 3 (7%) were aged 3 years, 5 (11.6%) were aged 4 years, 6 (14%) were aged 5 years, 6 (14%) were aged 6-9 years, and 7 (16.2%) were aged 10-15 years. We detected plural viruses, including rhinovirus, human metapneumovirus, enterovirus, cytomegalovirus, and adenovirus in 11 cases. Among the 32 HPIV4-only cases, 25 (78.1%) were diagnosed as nasopharyngitis, 5 (15.6%) as bronchitis, and others as laryngitis and viral exanthema.

A number of HPIV1-3 strains have been isolated with our surveillance system using the microplate method (12); however, HPIV4 strains have been rarely isolated. A local outbreak of HPIV4 was observed for the first time during the winter season of 2011-2012, as described here. Since the number of reported cases of HPIV4 in Japan is quite limited (9), few HPIV4-associated outbreaks have been observed apart from that presentated by Watanabe et al. (13). Even worldwide,

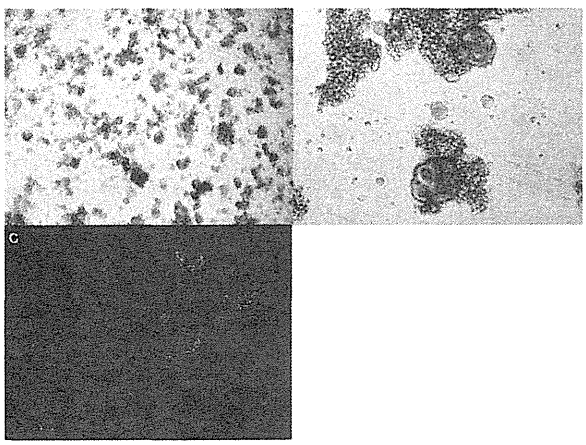

Fig. 1. Cytopathic effect and immunofluorescent staining of HPIV4 strains isolated from children with acute respiratory infection. Syncytia formation was observed on LLC-MK2 cell line (A) and on HMV-II cell line (B). The HPIV4-inoculated cells were stained using the indirect immunofluorescent method (C).

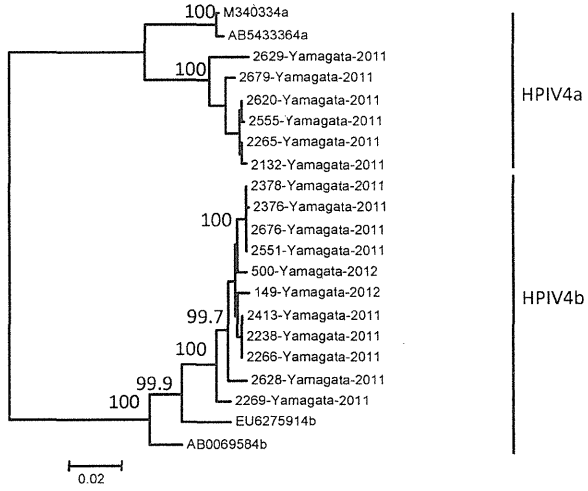

Fig. 3. Phylogenetic tree for the partial (1599 bp) sequence of the HN regions of HPIV4 strains detected in Yamagata, Japan between 2011 and 2012 as well as for the reference strains (GenBank accession numbers are shown). The numbers near the branches are the bootstrap probabilities (%).

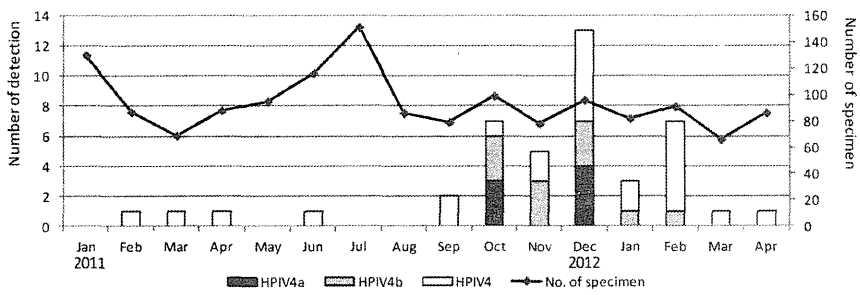

Fig. 2. Monthly distribution of acute respiratory infections associated with human parainfluenza virus type 4 (HPIV4) in children between January 2011 and April 2012 in Yamagata, Japan.

the number of HPIV4 cases reported is quite limited. Laurichesse et al. and Fry et al. reported that the number of HPIV4-positive cases was markedly smaller than that of HPIV1-3-positive cases (5,15). Lau et al. reported 41 HPIV4 cases during an outbreak in a developmental disability unit and 35 cases (1.2%) among 2,912 nasopharyngeal aspirates in a 1-year study (16,17); Ren et al. described 25 (10.2%) HPIV4 cases among 246 HPIV-positive cases over a 3-year period (6). Finally, Scott et al. described 13 HPIV4-positive cases, most of which were severe cases, during their 6-year study (7). Thus, our study experience together with the limited data, indicates the difficulties associated with the isolation and detection of HPIV4. To clarify the etiology and epidemiology of HPIV4 infections, HPIV4 infections should be recognized as common diseases that require active surveillance using sensitive cell lines such as LLC-MK2, as well as combining molecular method such as RT-PCR.

Watanabe et al. conducted an epidemiological study of HPIV4 among children with ARIs in Sendai and Yamagata. They isolated HPIV4 from 129 (0.8%) of 16,187 clinical specimens using the LLC-MK2 cell line between 2003 and 2009, and they commonly isolated HPIV4 during autumn (13). Based on their study, we believe that a number of HPIV4 infections in Yamagata were missed, especially those during the autumn season. Vachon et al. suggested that HPIV4 infections can be relatively common during the autum and winter seasons (18); Billaud et al. reported that they detected 18 of 20 HPIV4-positive cases during the autumn and winter (8). Now that we have succeeded in isolating and detecting HPIV4, we hope to determine if HPIV4 outbreaks commonly occur during autumn. Watanabe et al. also stated that approximately two-thirds of HPIV4-positive patients were diagnosed with lower respiratory infections such as pneumonia, bronchiolitis, and bronchitis (13). However, we found only 5 cases of bronchitis, and most of the patients in our study were diagnosed with nasopharyngitis. Thus, the clinical picture of HPIV4 remains controversial.

In conclusion, epidemiological data on HPIV4 are still quite limited and further studies are needed to clarify the etiology and epidemiology of HPIV4 infections.

Acknowledgments We thank the medical staff and people of Yamagata Prefecture for their collaboration in specimen collection for the surveillance of viral infectious diseases.

This work was supported by a grant-in-aid from the Japan Society for the Promotion of Science and for Research on Emerging and Re-emerging Infectious Diseases of the Ministry of Health, Labour and Welfare, Japan.

Conflict of interest None to declare.

REFERENCES

1. Psarras, S., Papadopoulos, N.G. and Johnston, S.L. (2009): Parainfluenza viruses. p. 409-439. *In* A.J. Zuckerman, J.E. Banatvala, B.D. Schoub, et al. (ed.), Principle & Practice of Clinical Virology. Wiley-Blackwell, West Sussex, United Kingdom.
2. Glezen, W.P. and Denny, F.W. (1997): Parainfluenza viruses. p. 551-567. *In* A.S. Evans and R.A. Kaslow (ed.), Viral Infections of Humans. Plenum Medical Book Company, New York.
3. Boyer, K.M. (2009): Non bacterial pneumonia. p. 288-301. *In* R.D. Feigin, J.D. Cherry, G.J. Demmler-Harrison, et al. (ed), Textbook of Pediatric Infectious Diseases. 6th ed. Saunders Elsevier, Philadelphia.
4. Robinson, C.C. (2009): Respiratory viruses. p. 203-248. *In* S. Specter, R.L. Hodinka, S.A. Young, et al. (ed), Clinical Virology Manual. 4th ed. ASM press, Washington, D.C.
5. Laurichesse, H., Dedman, D., Watson, J.M., et al. (1999): Epidemiological features of parainfluenza virus infections: laboratory surveillance in England and Wales, 1975-1977. Eur. J. Epidemiol., 15, 475-484.
6. Ren, L., Gonzalez, R., Xie, Z., et al. (2011): Human parainfluenza virus type 4 infection in Chinese children with lower respiratory tract infections: a comparison study. J. Clin. Virol., 51, 209-212.
7. Scott, L., Asha, D., Allison, I., et al. (1997): Parainfluenza virus type 4 infections in pediatric patients. Pediatr. Infect. Dis. J., 16, 34-38.
8. Billaud, G., Morfin, F., Vabret, A., et al. (2005): Human parainfluenza virus type 4 infections: a report of 20 cases from 1998 to 2002. J. Clin. Virol., 34, 48-51.
9. National Epidemiological Surveillance of Infectious Diseases (NESID) system. Online at <https://nesid3g.wish.mhlw.hq.admix.go.jp/GKWeb/GKMainServlet?action_id=GKMainMenu>. Accessed 27 June 2012.
10. Mizuta, K., Abiko, C., Aoki, Y., et al. (2008): Analysis of monthly isolation of respiratory viruses from children by cell culture using a microplate method: a two-year study from 2004 to 2005 in Yamagata, Japan. Jpn. J. Infect. Dis., 61, 196-201.
11. Mizuta, K., Saitoh, M., Kobayashi, M., et al. (2011): Detailed genetic analysis of hemagglutinin-neuraminidase glycoprotein gene in human parainfluenza virus type 1 isolates from patients with acute respiratory infection between 2002 and 2009 in Yamagata Prefecture, Japan. Virol. J., 8, 533.
12. Mizuta, K., Abiko, C., Aoki, Y., et al. (2012): Epidemiology of parainfluenza virus type 1, 2 and 3 infections based on virus isolation between 2002 and 2011 in Yamagata, Japan. Microbiol. Immunol., 56, 855-858.
13. Watanabe, O., Ohmi, A., Nagai, Y., et al. (2011): Abstract 32. 65th Annual Meeting of Tohoku Society of Microbiology. Online at <http://minfo.id.yamagata-u.ac.jp/Imm/65bact/img/shouroku.pdf> (in Japanese).
14. Tong, S., Chern, S.W., Li, Y., et al. (2008): Sensitive and broadly reactive reverse transcription-PCR assays to detect novel paramyxoviruses. J. Clin. Microbiol., 46, 2652-2658.
15. Fry, A.M., Curns, A.T., Harbour, K., et al. (2006): Seasonal trends of human parainfluenza viral infections: United States, 1990-2004. Clin. Infect. Dis., 43, 1016-1022.
16. Lau, S.K.P., To, W., Tse, P.W.T., et al. (2005): Human parainfluenza virus type 4 outbreak and the role of diagnostic tests. J. Clin. Microbiol., 43, 4515-4521.
17. Lau, S.K.P., Li, K.S.M., Chau, K., et al. (2009): Clinical and molecular epidemiology of human parainfluenza virus 4 infections in Hong Kong: subtype 4B as common as subtype 4A. J. Clin. Microbiol., 47, 1549-1552.
18. Vachon, M., Dionne, N., Leblanc, E., et al. (2006): Human parainfluenza type 4 infections, Canada. Emerg. Infect. Dis., 12, 1755-1758.

Journal of Clinical Microbiology

Genetic Analysis of Non-Hydrogen Sulfide-Producing Salmonella enterica Serovar Typhimurium and S. enterica Serovar Infantis Isolates in Japan

Chieko Sakano, Makoto Kuroda, Tsuyoshi Sekizuka, Taisei Ishioka, Yukio Morita, Akihide Ryo, Hiroyuki Tsukagoshi, Yuko Kawai, Nobuko Inoue, Hayato Takada, Yumiko Ogaswara, Atsuyoshi Nishina, Masa-aki Shimoda, Kunihisa Kozawa, Kazunori Oishi and Hirokazu Kimura

J. Clin. Microbiol. **2013, 51(1):328. DOI: 10.1128/JCM.02225-12.**
Published Ahead of Print 7 November 2012.

JCM
Journals.ASM.org

Genetic Analysis of Non-Hydrogen Sulfide-Producing *Salmonella enterica* Serovar Typhimurium and *S. enterica* Serovar Infantis Isolates in Japan

Chieko Sakano,[a] Makoto Kuroda,[b] Tsuyoshi Sekizuka,[b] Taisei Ishioka,[a] Yukio Morita,[a,c] Akihide Ryo,[d] Hiroyuki Tsukagoshi,[a] Yuko Kawai,[a] Nobuko Inoue,[a] Hayato Takada,[a] Yumiko Ogaswara,[b] Atsuyoshi Nishina,[e] Masa-aki Shimoda,[a] Kunihisa Kozawa,[a] Kazunori Oishi,[f,g] Hirokazu Kimura[a,f]

Gunma Prefectural Institute of Public Health and Environmental Sciences, Maebashi-shi, Gunma, Japan[a]; Pathogen Genomics Center, National Institute of Infectious Diseases, Toyama, Shinjuku-ku, Tokyo, Japan[b]; College of Nutritional Science, Tokyo Kasei University, Kaga, Itabashi-ku, Tokyo, Japan[c]; Department of Molecular Biodefense Research, Yokohama City University Graduate School of Medicine, Fukuura, Kanazawa-ku, Yokohama, Kanagawa, Japan[d]; Yamagata Prefectural Yonezawa Women's Junior College, Yonezawa-shi, Yamagata, Japan[e]; Infectious Disease Surveillance Center, National Institute of Infectious Diseases, Gakuen, Musashimurayama-shi, Tokyo, Japan[f]; Infectious Disease Surveillance Center, National Institute of Infectious Diseases, Toyama, Shinjuku-ku, Tokyo, Japan[g]

Whole-genome sequencing of non-H_2S-producing *Salmonella enterica* serovar Typhimurium and *S. enterica* serovar Infantis isolates from poultry meat revealed a nonsense mutation in the *phsA* thiosulfate reductase gene and carriage of a CMY-2 β-lactamase. The lack of production of H_2S might lead to the incorrect identification of *S. enterica* isolates carrying antimicrobial resistance genes.

Salmonella enterica subsp. *enterica* serovar Typhimurium and *S. enterica* serovar Infantis of the genus *Salmonella* cause acute enterocolitis. Generally, H_2S production is considered to be indicative of the presence of pathogenic food-borne *Salmonella* serovars and is an important index for screening and confirmation of *Salmonella* using various agars, including DHL (deoxycholate hydrogen sulfide lactose), SS (*Salmonella-Shigella*), and TSI (triple sugar iron) agars.

We isolated non-H_2S-producing *S.* Typhimurium and *S.* Infantis strains from retail chicken meats in Gunma prefecture, Japan, in 2010. Forty-seven *Salmonella* spp. isolates were obtained from 95 poultry meat samples (49.5%) between June and December 2010. Four (8.5%) were non-H_2S-producing *Salmonella* (*S.* Typhimurium isolates GST-106, GST-108, and GST-204; *S.* Infantis isolate GSI-9) isolates. H_2S production and lysine decarboxylase testing of *Salmonella* on TSI and LIM (lysine indole motility) agar was subsequently conducted (see Fig. S1 in the supplemental material). The other isolates found to be H_2S producing were as follows: *S. enterica* serovar Enteritidis (1 strain), *S. enterica* serovar Yovokome (1 isolate), *S. enterica* serovar Livingstone (1 isolate), *S. enterica* serovar Schwarzengrund (3 isolates), *S. enterica* serovar Manhattan (3 isolates), *S.* Infantis (38 isolates), and *S.* Typhimurium (2 isolates).

Pulsed-field gel electrophoresis (PFGE) analysis (1) suggested that the profile of the *S.* Infantis and *S.* Typhimurium strains were similar but not identical among these serovars (see Fig. S2 in the supplemental material). Multilocus sequence typing (MLST) for *S. enterica* (http://mlst.ucc.ie/mlst/dbs/Senterica/) suggested that the *S.* Typhimurium strains belonged to ST328, while the *S.* Infantis strains belonged to ST32 (see Table S1 in the supplemental material).

To elucidate the genetic alteration responsible for H_2S production, Illumina GAIIx 81-mer paired-end short read sequencing of *S.* Infantis and *S.* Typhimurium isolates was performed (see Table S1 in the supplemental material), followed by short-read mapping (2) against the corresponding reference genome sequences of *S.* Infantis SIN (downloaded from the Wellcome Trust Sanger Institute [ftp://ftp.sanger.ac.uk/pub/pathogens/Salmonella/SIN.dbs]) and *S.* Typhimurium T000240 (3), respectively. Whole-genome sequencing suggested that some nucleotide variations were present between H_2S-producing and non-H_2S-producing isolates (see Tables S2 and S3 in the supplemental material). Notably, the *phsA* gene, encoding the thiosulfate reductase precursor, was terminated in the coding sequence by an alteration to the stop codon (nonsense mutation) in both *S.* Infantis (GSI-9) and *S.* Typhimurium (GST-106, GST-108 and GST-204) (Fig. 1; also, see Tables S2 and S3 in the supplemental material). The *phs* genes are essential for the dissimilatory anaerobic reduction of thiosulfate to H_2S in *S.* Typhimurium (4, 5), suggesting that the disruption of the *phsA* gene could be involved in H_2S production. Intriguingly, a nonsense mutation in the *phsA* gene was also identified in low-H_2S-producing *S. enterica* serovar Paratyphi A (AKU_12601 and ATCC 9150) (6); thus, comparative genomic analysis also supports our findings.

H_2S is highly toxic to mammalian cells, including those of humans, and the cecal mucosa detoxifies H_2S by converting it to thiosulfate ($S_2O_3^-$) (7). Luminal inflammation generates reactive oxygen species, leading to the conversion of thiosulfate to tetrathionate ($S_4O_6^{2-}$). *S. enterica* utilizes tetrathionate as an electron acceptor in anaerobic respiration using TtrABC and TtrRS located on a SPI2 pathogenicity island (8). It is possible that non-H_2S-

Received 20 August 2012 **Returned for modification** 11 September 2012
Accepted 27 October 2012
Published ahead of print 7 November 2012
Address correspondence to Hirokazu Kimura, kimhiro@nih.go.jp, or Makoto Kuroda, makokuro@nih.go.jp.
Supplemental material for this article may be found at http://dx.doi.org/10.1128/JCM.02225-12.

doi:10.1128/JCM.02225-12

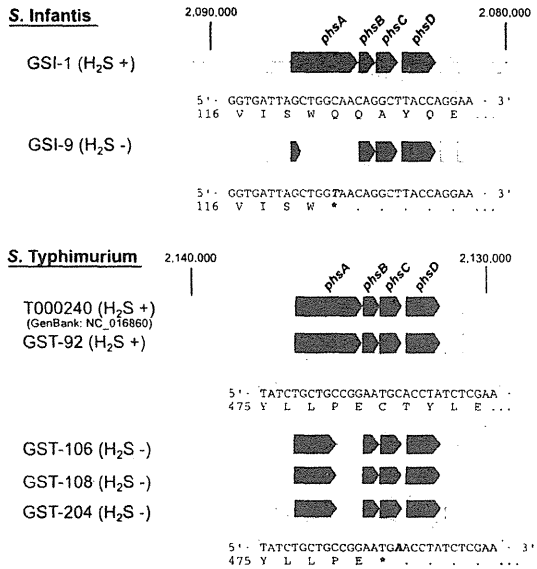

FIG 1 Schematic representation of the nonsense mutation in the *phsA* gene encoding the thiosulfate reductase subunit. Nucleotide variations and corresponding amino acid mutations are shown below the gene organization schemes.

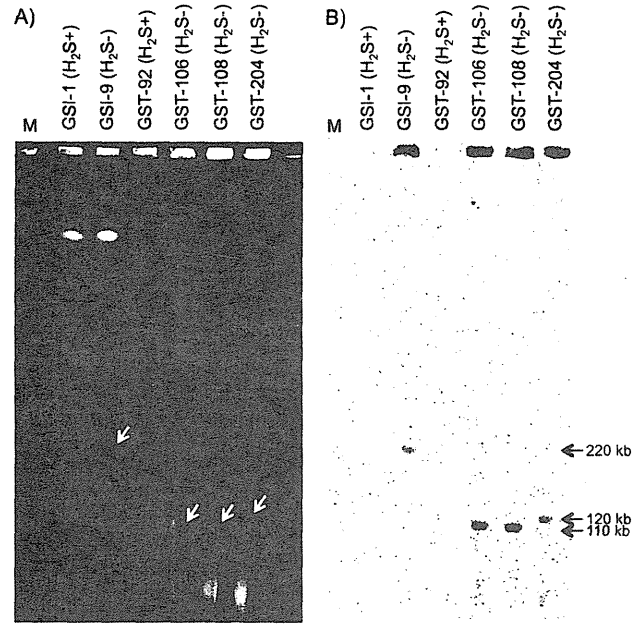

FIG 2 PFGE-Southern blot hybridization for bla_{CMY-2} detection. (A) S1 nuclease-PFGE analysis of the *Salmonella* isolates. (B) Southern blot obtained using a bla_{CMY-2}-specific DNA probe. M, lambda ladder marker for PFGE.

producing phenotypes generate more thiosulfate, leading to enough substrate for TtrABCRS anaerobic respiration in *Salmonella* spp. Indeed, recent studies have suggested that TtrABCRS anaerobic respiration based on tetrathionate contributes to competitiveness with other microbiota in intestinal inflammation (9, 10, 11), implying that reduced H_2S production might lead to increased TtrABCRS anaerobic respiration that promotes growth and colonization in the gut.

Furthermore, the non-H_2S-producing *S.* Infantis and *S.* Typhimurium isolates carried CMY-2 β-lactamase (Table 1) and demonstrated reduced susceptibility to cefazolin (data not shown). Aminoglycoside and trimethoprim resistance genes were also identified (Table 1). A plasmid carrying the bla_{CMY-2} gene was detected by S1 nuclease–PFGE and Southern blot analysis (12), indicating that it appears to have been an independent acquisition by two different serovars (Fig. 2). The CMY enzyme is the enzyme most frequently detected in *E. coli*, *Klebsiella pneumoniae*, and *Salmonella* spp. (13), and poultry meat is most frequently contaminated with CMY-2-producing *Salmonella* (14). Indeed, CMY-2-producing *S.* Infantis and *S.* Typhimurium isolates have been found in retail chicken and cattle in Japan (15, 16). Because of the clinical importance of third- and fourth-generation cephalosporin in human and veterinary medicine, it is of further concern that insufficient testing might lead to antimicrobial-resistant *Salmonella* isolates being missed.

In conclusion, we isolated non-H_2S-producing *S. enterica* isolates. Whole-genome analysis suggested that this lack of H_2S production may be associated with a *phsA* gene mutation and that these strains may be disseminated in poultry. Although we did not examine the pathogenicity of these strains in experimental animals, this defect may be associated with energy production and gut colonization. In addition, such strains may slip unnoticed past screening methods, resulting in incorrect identification of *S. enterica*, including antimicrobial resistant isolates. Comprehensive testing will be required to detect unique isolates and to map the overall epidemiology of *S. enterica*.

Nucleotide sequence accession number. Obtained short reads have been deposited in the DDBJ Sequence Read Archive of Japan (accession number DRA000592).

TABLE 1 Antimicrobial resistance genes in *Salmonella* isolates[a]

Isolate	Aminoglycosides			β-Lactams		Tetracycline—*tet*(B)	Trimethoprim—*dfrA14*
	aadA1	*aac(6')-Iaa*	*aph(3')-Ic*	bla_{CMY-2}	bla_{TEM-1}		
GSI-1 (H_2S^+)	+	−	−	−	−	−	+
GSI-9 (H_2S^-)	−	+	−	+	−	−	−
GST-92 (H_2S^+)	+	+	+	−	+	−	+
GST-106 (H_2S^-)	−	+	−	+	−	+	−
GST-108 (H_2S^-)	−	+	−	+	−	+	−
GST-204 (H_2S^-)	−	+	−	+	−	+	−

[a] Antimicrobial resistance genes were identified in a ResFinder web search (http://www.cbs.dtu.dk/services/ResFinder/).

ACKNOWLEDGMENT

This work was supported by a Grant-in-Aid from the Ministry of Health, Labor, and Welfare, Japan (H24 Shokuhin-Ippan-008).

REFERENCES

1. Gerner-Smidt P, Hise K, Kincaid J, Hunter S, Rolando S, Hyytia-Trees E, Ribot EM, Swaminathan B. 2006. PulseNet U. S. A.: a five-year update. Foodborne Pathogens Dis. 3:9–19.
2. Li H, Durbin R. 2010. Fast and accurate long-read alignment with Burrows-Wheeler transform. Bioinformatics 26:589–595.
3. Izumiya H, Sekizuka T, Nakaya H, Taguchi M, Oguchi A, Ichikawa N, Nishiko R, Yamazaki S, Fujita N, Watanabe H, Ohnishi M, Kuroda M. 2011. Whole-genome analysis of *Salmonella enterica* serovar Typhimurium T000240 reveals the acquisition of a genomic island involved in multidrug resistance *via* IS1 derivatives on the chromosome. Antimicrob. Agents Chemother. 55:623–630.
4. Clark MA, Barrett EL. 1987. The phs gene and hydrogen sulfide production by *Salmonella* typhimurium. J. Bacteriol. 169:2391–2397.
5. Alami N, Hallenbeck PC. 1992. Mutations that affect the regulation of phs in *Salmonella* typhimurium. J. Gen. Microbiol. 138:1117–1122.
6. McClelland M, Sanderson KE, Clifton SW, Latreille P, Porwollik S, Sabo A, Meyer R, Bieri T, Ozersky P, McLellan M, Harkins CR, Wang C, Nguyen C, Berghoff A, Elliott G, Kohlberg S, Strong C, Du Carter F J, Kremizki C, Layman D, Leonard S, Sun H, Fulton L, Nash W, Miner T, Minx P, Delehaunty K, Fronick C, Magrini V, Nhan M, Warren W, Florea L, Spieth J, Wilson RK. 2004. Comparison of genome degradation in Paratyphi A and Typhi, human-restricted serovars of *Salmonella enterica* that cause typhoid. Nat. Genet. 36:1268–1274.
7. Levitt MD, Furne J, Springfield J, Suarez F, DeMaster E. 1999. Detoxification of hydrogen sulfide and methanethiol in the cecal mucosa. J. Clin. Invest. 104:1107–1114.
8. Hensel M, Hinsley AP, Nikolaus T, Sawers G, Berks BC. 1999. The genetic basis of tetrathionate respiration in *Salmonella* typhimurium. Mol. Microbiol. 32:275–287.
9. Winter SE, Thiennimitr P, Winter MG, Butler BP, Huseby DL, Crawford RW, Russell JM, Bevins CL, Adams LG, Tsolis RM, Roth JR, Baumler AJ. 2010. Gut inflammation provides a respiratory electron acceptor for *Salmonella*. Nature 467:426–429.
10. Thiennimitr P, Winter SE, Winter MG, Xavier MN, Tolstikov V, Huseby DL, Sterzenbach T, Tsolis RM, Roth JR, Baumler AJ. 2011. Intestinal inflammation allows *Salmonella* to use ethanolamine to compete with the microbiota. Proc. Natl. Acad. Sci. U. S. A. 108:17480–17485.
11. Rohmer L, Hocquet D, Miller SI. 2011. Are pathogenic bacteria just looking for food? Metabolism and microbial pathogenesis. Trends Microbiol. 19:341–348.
12. Shahada F, Sekizuka T, Kuroda M, Kusumoto M, Ohishi D, Matsumoto A, Okazaki H, Tanaka K, Uchida I, Izumiya H, Watanabe H, Tamamura Y, Iwata T, Akiba M. 2011. Characterization of *Salmonella enterica* serovar Typhimurium isolates harboring a chromosomally encoded CMY-2 β-lactamase gene located on a multidrug resistance genomic island. Antimicrob. Agents Chemother. 55:4114–4121.
13. Li XZ, Mehrotra M, Ghimire S, Adewoye L. 2007. β-Lactam resistance and β-lactamases in bacteria of animal origin. Vet. Microbiol. 121:197–214.
14. Arlet G, Barrett TJ, Butaye P, Cloeckaert A, Mulvey MR, White DG. 2006. *Salmonella* resistant to extended-spectrum cephalosporins: prevalence and epidemiology. Microbes Infect. 8:1945–1954.
15. Taguchi M, Seto K, Yamazaki W, Tsukamoto T, Izumiya H, Watanabe H. 2006. CMY-2 β-lactamase-producing *Salmonella enterica* serovar Infantis isolated from poultry in Japan. Jpn. J. Infect. Dis. 59:144–146.
16. Sugawara M, Komori J, Kawakami M, Izumiya H, Watanabe H, Akiba M. 2011. Molecular and phenotypic characteristics of CMY-2 β-lactamase-producing *Salmonella enterica* serovar Typhimurium isolated from cattle in Japan. J. Vet. Med. Sci. 73:345–349.

Jpn. J. Infect. Dis., 66, 56-59, 2013

Short Communication

Molecular Epidemiology of Human Metapneumovirus from 2005 to 2011 in Fukui, Japan

Masako Nakamura[1], Eiko Hirano[1], Fubito Ishiguro[1], Katsumi Mizuta[2], Masahiro Noda[3], Ryota Tanaka[4], Hiroyuki Tsukagoshi[5]*, and Hirokazu Kimura[3]

[1]*Fukui Prefectural Institute of Public Health and Environmental Science, Fukui 910-8551;*
[2]*Yamagata Prefectural Institute of Public Health, Yamagata 990-0031;*
[3]*Infectious Disease Surveillance Center, National Institute of Infectious Diseases, Tokyo 208-0011;*
[4]*Department of Surgery, Kyorin University School of Medicine, Tokyo 181-8611; and*
[5]*Gunma Prefectural Institute of Public Health and Environmental Sciences, Gunma 371-0052, Japan*

(Received June 22, 2012. Accepted October 5, 2012)

SUMMARY: To investigate the molecular epidemiology of human metapneumovirus (HMPV) infections in acute respiratory infections (ARI), we performed genetic analysis of the *F* gene in HMPV from patients with ARI in Fukui Prefecture from August 2005 to July 2011. HMPV was detected in 53 of 741 nasopharyngeal swabs (7.2%). Phylogenetic analysis helped us assign 31 strains to subgroup A2, 1 strain to subgroup B1, and 21 strains to subgroup B2. The prevalence of HMPV was peaked between January and June. A high degree of nucleotide identity was seen among subgroup A2 strains (95.6–100%) and subgroup B2 strains (97.5–100%). In addition, no positively selected sites (substitutions) were found in the *F* gene in these HMPV strains. The results suggest that the prevalent HMPV strains in Fukui were associated with various ARI in Japan during the investigation period.

Human metapneumovirus (HMPV), which belongs to the family *Paramyxoviridae*, genus *Metapneumovirus*, is an important cause of acute respiratory infections (ARI) in humans (1). Higher morbidity is observed in young children, the elderly, and immunocompromised people (2,3). Indeed, HMPV infection in some infants and the elderly may result in severe ARI such as bronchiolitis and bronchopneumonia (4,5).

HMPV is classified into two genotypes (A and B) and four subgroups (A1, A2, B1, and B2) by phylogenetic analysis (6,7). It has been suggested that these genotypes circulate in variable proportions in some areas (8,9). Although information available for HMPV molecular epidemiology has been gradually accumulated, the epidemiology of HMPV remains unclear (4,10). In this study, we performed genetic analysis of the fusion (*F*) gene of HMPV from patients with ARI in Fukui Prefecture from August 2005 to July 2011 to investigate the molecular epidemiology of HMPV infections.

Throat swab samples were collected from 741 patients (age range, 0–100 years; mean ± standard deviation [SD], 14.6 ± 29.2 years) with ARI at clinics collaborating with the local health authority of Fukui Prefecture in the surveillance of viral diseases in Japan. Informed consent was obtained from the subjects or assent was obtained from their parents for the donation of throat swab samples. The study comprised 584 patients aged 0–5 (1.46 ± 1.32 years), 33 patients aged 6–12 (7.85 ± 2.03 years), and 124 patients aged 13–100 years (76.7 ± 17.5 years). Of the 741 patients, 170 were diagnosed with upper respiratory infections (URI) and 396 with lower respiratory infections (LRI), including bronchitis and pneumonia.

We tried to detect influenza virus, human rhinovirus, enteroviruses, respiratory syncytial virus, and adenoviruses using reverse transcriptase-polymerase chain reaction (RT-PCR) and cell culture methods (Vero E6, RD, MDCK, and HEp-2 cells) (11–14). Viral nucleic acid was extracted from the samples using the MinElute Virus Spin Kit or EZ1 Virus Mini Kit v2.0 (QIAGEN, Valencia, Calif., USA) and suspended in DNase/RNase-free water. After RNA extraction, nested RT-PCR was performed as previously described (4,15). Amplicons were purified using a QIAquick PCR Purification Kit (QIAGEN) and the nucleotide sequences were determined by direct sequencing (4,15). Sequence data were registered under the accession nos. AB716360–AB716412 at GenBank. Next, we performed phylogenetic analysis based on partial *F* gene (position: 3783–4099 of strain NL/1/99) of the most frequently analyzed HMPV strains using Molecular Evolutionary Genetics Analysis (MEGA) software version 4 (16). Evolutionary distances were estimated using Kimura's two-parameter method, and a phylogenetic tree was constructed using the neighbor-joining method (17,18). The reliability of the tree was estimated using 1,000 bootstrap replications. In addition, we calculated the pairwise distances for the present strains to assess the frequency distribution of HMPV genotypes A and B, as previously described (6,7,19). Furthermore, positive selections were identified using DATAMONKEY (http://www.datamonkey.org) (20). We used the following four methods to estimate the synonymous (dS) and non-synonymous (dN) rates at every codon in the alignment: single likelihood ancestor counting (SLAC); fixed effects likelihood (FEL); and internal fixed effects likeli-

*Corresponding author: Mailing address: Gunma Prefectural Institute of Public Health and Environmental Sciences, Tel: +81-27-232-4881, Fax: +81-27-234-8438, E-mail: tsuka-hiro@pref.gunma.lg.jp

Table 1. Subject data in this study

Year	No. of samples	HMPV positive /subgroup, no. of patients	Diagnosis reported in HMPV positive patients				
			URI	Wheezy bronchitis	ILI	Pneumonia	Others
2005	20	1/A2		1			
		1/B2			1		
2006	155	6/A2		5	1		
		5/B2		3	2		
2007	144	8/A2	2	6			
		1/B1		1			
		4/B2	1	1			2
2008	214	3/A2	1	2			
		8/B2	3	3		1	1
2009	66	2/A2		2			
		2/B2		2			
2010	94	1/A2	1				
2011	48	10/A2	2	4			4
		1/B2		1			
Total	741	53	10	31	4	1	7[1)]

[1)]: Unknown fever 3, conjunctivitis 1, gastroenteritis 1, unknown 2.
URI, upper respiratory infection; ILI, influenza like illness.

hood (IFEL). SLAC, FEL, and IFEL methods detect sites under selection at external branches of the phylogenetic tree, and the IFEL method investigates sites along the internal branches. Positive selection (dN > dS) was determined by a *P*-value of <0.1 (SLAC, FEL, IFEL).

A summary of patient and viral data is shown in Table 1. HMPV was detected in 53 of 741 (7.2%) patients with ARI during the investigation period. The age of the 53 HMPV-positive patients was 7.1 ± 18.4 years. Of the 53 detected, 48 (90.6%) were found in samples from patients under 5 years of age. No other viruses were detected in these patients. Notably, over 60% of the patients were clinically diagnosed with wheezy bronchitis.

In this study, HMPV was found to be prevalent from January to June (Fig. 1). Previous studies have suggested that HMPV is prevalent during the winter-spring season in many countries, including Japan (10). Indeed, Mizuta et al. showed that the peak season for HMPV is from winter to spring (between January and May) and the low season is during fall (around September and October) (10). Thus, the findings of the present study are in agreement with those of the previous study (10).

The phylogenetic tree based on the partial nucleotide sequence of the partial *F* gene (317 bp) is shown in Fig. 2. Of the 53 HMPV strains, 31 and 22 were classified as genotypes A and B, respectively. All strains belonging to genotype A were assigned to subgroup A2 and 1 strain belonging to genotype B was assigned to subgroup B1, while the other 21 strains were assigned to subgroup B2. The nucleotide identity among the present strains was 83.9–100%. Although there were some differences, a high degree of nucleotide identity was seen among subgroup A2 strains (95.6–100%) and subgroup B2 strains (97.5–100%), as indicated in a previous report (21). The pairwise distance values among the present strains belonging to subgroup A2 were 0.019 ± 0.013 and those of subgroup B2 were 0.014 ± 0.008.

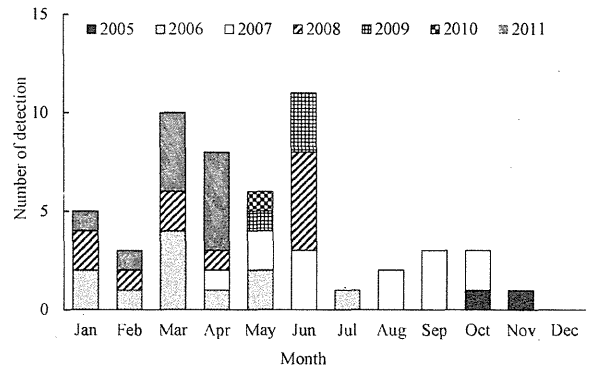

Fig. 1. Seasonal variations in HMPV infection.

Pairwise distance values based on the nucleotide sequences among the present strains were relatively low (<0.02). In addition, we did not observe any evidence of positive selection. These results suggest that a highly conserved partial *F* coding region in HMPV was prevalent in Fukui Prefecture, Japan. In addition, we found that most of the nucleotide substitutions of the *F* gene were synonymous in the present strains. Based on these data, the dN/dS ratios of all substitutions were synonymous. Thus, no positively selected sites were found in the present strains. There were 30 common sites under negative selection as identified by SLAC, FEL, and IFEL methods. To our best knowledge, it is not known if these negatively selected sites are involved in immune responses and viral functions. However, F protein is the major antigenic determinant of protection (22). Therefore, we consider these negatively selected sites as potential players in viral functions, host immunity, and vaccine development.

A previous longitudinal epidemiological study suggested that subgroups A2 and B2 were predominant in Yamagata Prefecture, Japan, from 2004 to 2009 (10). In

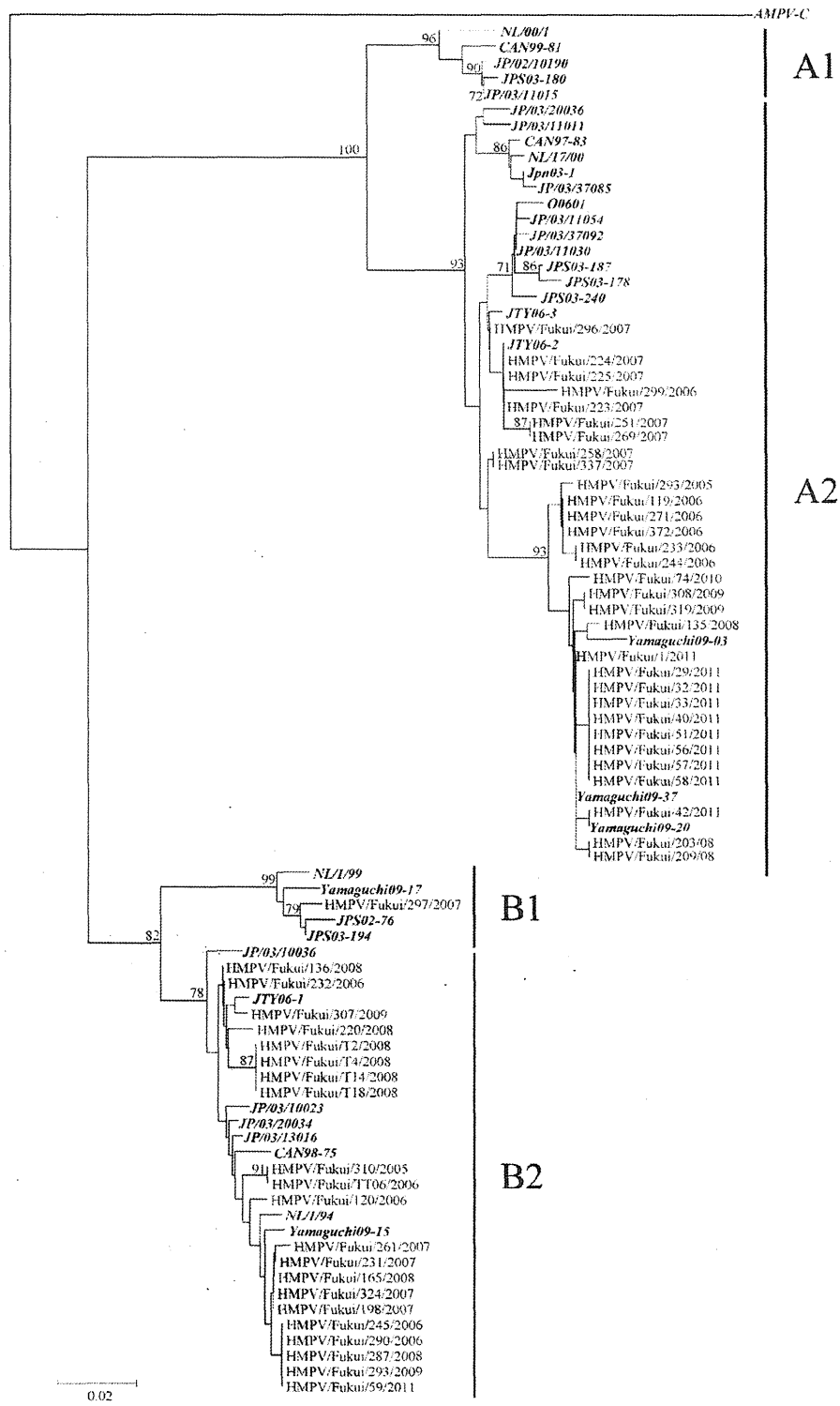

Fig. 2. Phylogenetic tree constructed on the basis of partial sequences of human metapneumovirus partial *F* gene (317 bp). Distances were calculated using Kimura's two-parameter method, and the tree was plotted using the neighbor-joining method. Numbers above the branches are bootstrap probabilities (%). Reference strains were NL/00/1 (AF371337), CAN99-81 (AY145294), JP/02/10190 (AB113377), JP/03/11015 (AB113372), JPS03-180 (AY530092), CAN97-83 (AY145296), NL/17/00 (AY304360), Jpn03-1 (AB503857), JP/03/37085 (AB119485), JP/03/11011 (AB113371), JP/03/20036 (AB126612), JTY06-2 (EU127918), JTY06-3 (EU127919), JP/03/37092 (AB119486), JP/03/11030 (AB119489), JP/03/11054 (AB119491), JPS03-240 (AY530095), O0601 (EF589610), JPS03-187 (AY530093), JPS03-178 (AY530091), Yamaguchi09-37 (AB533251), Yamaguchi09-20 (AB533245), Yamaguchi09-03 (AB533239), NL/1/99 (AY304361), Yamaguchi09-17 (AB533244), JPS02-76 (AY530089), JPS03-194 (AY530094), JP/03/10036 (AB126611), JTY06-1 (EU127917), JP/03/10023 (AB126608), JP/03/20034 (AB119493), CAN98-75 (AY297748), JP/03/13016 (AB126607), NL/1/94 (AY304362), and Yamaguchi09-15 (AB533243). Avian metapneumovirus type C (AMPV-C [AY579780]) was also included as an outgroup.

addition, these subgroups have been found to be predominant in other studies (4,21). Our results appear to be compatible with these previous studies (4,10,21). Furthermore, we performed partial *F* gene analysis for subgroups A2, B1, and B2, and found a high level of sequence identity (95.6–100%). These results were almost identical to a previous report (93.5–97.6%) (23). Our data support the theory that F protein is relatively well conserved.

In this study, we did not perform bacteriological examinations by culture-based methods or PCR detection of major respiratory pathogens. Therefore, we could not exclude co-infection with respiratory pathogens.

In conclusion, HMPV strains detected in samples from patients with ARI during 2005–2011 in Fukui Prefecture, Japan showed a high degree of genetic identity. Our results indicated that subgroups A2 and B2 were predominant. These HMPV strains might be associated with various ARI in Japan during the investigation period. However, additional epidemiological studies are needed to gain a better understanding of HMPV in other areas of Japan.

Acknowledgments This work was supported in part by a Grant-in-Aid for Research on Emerging and Re-emerging Infectious Diseases, Labour and Welfare Programs from the Ministry of Health, Labour and Welfare of Japan.

Conflict of interest None to declare.

REFERENCES

1. Collins, P.L. and Crowe, J.E., Jr. (2007): Respiratory syncytial virus and metapneumovirus. p. 1601–1646. *In* D.M. Knipe and P.M. Howley (ed.), Fields Virology. vol. 1. 5th ed. Lippincott Williams & Wilkins, Philadelphia.
2. Falsey, A.R., Erdman, D., Anderson, L.J., et al. (2003): Human metapneumovirus infections in young and elderly adults. J. Infect. Dis., 187, 785–790.
3. Pelletier, G., Dery, P., Abed, Y., et al. (2002): Respiratory tract reinfections by the new human metapneumovirus in an immunocompromised child. Emerg. Infect. Dis., 8, 976–978.
4. Omura, T., Iizuka, S., Tabara, K., et al. (2011): Detection of human metapneumovirus genomes during an outbreak of bronchitis and pneumonia in a geriatric care home in Shimane, Japan, in autumn 2009. Jpn. J. Infect. Dis., 64, 85–87.
5. Boivin, G., De Serres, G., Hamelin, M.E., et al. (2007): An outbreak of severe respiratory tract infection due to human metapneumovirus in a long-term care facility. Clin. Infect. Dis., 44, 1152–1158.
6. van den Hoogen, B.G., Herfst, S., Sprong, L., et al. (2004): Antigenic and genetic variability of human metapneumoviruses. Emerg. Infect. Dis., 10, 658–666.
7. Biacchesi, S., Skiadopoulos, M.H., Boivin, G., et al. (2003): Genetic diversity between human metapneumovirus subgroups. Virology, 315, 1–9.
8. Gerna, G., Campanini, G., Rovida, F., et al. (2005): Changing circulation rate of human metapneumovirus strains and types among hospitalized pediatric patients during three consecutive winter-spring seasons. Brief report. Arch. Virol., 150, 2365–2375.
9. Mackay, I.M., Bialasiewicz, S., Jacob, K.C., et al. (2006): Genetic diversity of human metapneumovirus over 4 consecutive years in Australia. J. Infect. Dis., 193, 1630–1633.
10. Mizuta, K., Abiko, C., Aoki, Y., et al. (2010): Endemicity of human metapneumovirus subgenogroups A2 and B2 in Yamagata, Japan, between 2004 and 2009. Microbiol. Immunol., 54, 634–638.
11. Nakauchi, M., Yasui, Y., Miyoshi, T., et al. (2011): One-step real-time reverse transcription-PCR assays for detecting and subtyping pandemic influenza A/H1N1 2009, seasonal influenza A/H1N1, and seasonal influenza A/H3N2 viruses. J. Virol. Methods, 171, 156–162.
12. Savolainen, C., Blomqvist, S., Mulders, M.N., et al. (2002): Genetic clustering of all 102 human rhinovirus prototype strains: serotype 87 is close to human enterovirus 70. J. Gen. Virol., 83, 333–340.
13. Osiowy, C. (1998): Direct detection of respiratory syncytial virus, parainfluenza virus, and adenovirus in clinical respiratory specimens by a multiplex reverse transcription-PCR assay. J. Clin. Microbiol., 36, 3149–3154.
14. Aguilar, J.C., Pérez-Breña, M.P., García, M.L., et al. (2000): Detection and identification of human parainfluenza viruses 1, 2, 3, and 4 in clinical samples of pediatric patients by multiplex reverse transcription-PCR. J. Clin. Microbiol., 38, 1191–1195.
15. Takao, S., Shimozono, H., Kashiwa, H., et al. (2003): Clinical study of pediatric cases of acute respiratory diseases associated with human metapneumovirus in Japan. Jpn. J. Infect. Dis., 56, 127–129.
16. Tamura, K., Dudley, J., Nei, M., et al. (2007): MEGA4: Molecular Evolutionary Genetics Analysis (MEGA) software version 4.0. Mol. Biol. Evol., 24, 1596–1599.
17. Kimura, M. (1980): A simple method for estimating evolutionary rates of base substitution through comparative studies of nucleotide sequences. J. Mol. Evol., 16, 111–120.
18. Saitou, N. and Nei, M. (1987): The neighbor-joining method: a new method for reconstructing phylogenetic trees. Mol. Biol. Evol., 4, 406–425.
19. Mizuta, K., Hirata, A., Suto, A., et al. (2010): Phylogenetic and cluster analysis of human rhinovirus species A (HRV-A) isolated from children with acute respiratory infections in Yamagata, Japan. Virus Res., 147, 265–274.
20. Pond, S.L. and Frost, S.D. (2005): Datamonkey: rapid detection of selective pressure on individual sites of codon alignments. Bioinformatics, 21, 2531–2533.
21. Boivin, G., Mackay, I., Sloots, T.P., et al. (2004): Global genetic diversity of human metapneumovirus fusion gene. Emerg. Infect. Dis., 10, 1154–1157.
22. Cseke, G., Wright, D.W., Tollefson, S.J., et al. (2007): Human metapneumovirus fusion protein vaccines that are immunogenic and protective in cotton rats. J. Virol., 81, 698–707.
23. Yang, C., Wang, C.K., Tollefson, S.J., et al. (2009): Genetic diversity and evolution of human metapneumovirus fusion protein over twenty years. Virol. J., 6, 138.

Table 2 Distribution of the protection against diphtheria and tetanus (≥0.1 UI/mL) in the homeless population.

Immune status	All	No. (%) of donnors age group, years		
		<25	25–50	>50
Diphtheria protected[a]/ Tetanus protected[a]	62 (71.3)	5 (100)	29 (74.4)	28 (65.1)
Diphtheria protected[a]/ Tetanus unprotected[b]	12 (13.8)	0 (0)	4 (10.3)	8 (18.6)
Diphtheria unprotected[b]/ Tetanus protected[a]	7 (8.0)	0 (0)	3 (7.7)	4 (9.3)
Diphtheria unprotected[b]/ Tetanus unprotected[b]	6 (6.9)	0 (0)	3 (7.7)	3 (7.0)
Total	87 (100)	5 (100)	39 (100)	43 (100)

[a] Titer ≥0.1 UI/mL.
[b] Titer <0.1 UI/mL.

tetanus and diphtheria vaccine should be used, when a tetanus booster is required.

Funding

No funding was received for this study.

Conflict of interest

No conflicts of interest exist.

Acknowledgments

For their cooperation, we thank the medical and pharmacy students, interns, and fellows; researchers of the URMITE; the infectious diseases specialists who actively participated in the study. We also thank the directors and the staff of the 2 shelters.

References

1. Six C, Blanes de Canecaude J, Duponchel J, Lafont E, Decoppet A, Travanut M, et al. Spotlight on measles 2010: measles outbreak in the Provence-Alpes-Côte d'Azur region, France, January to November 2010-substantial underreporting of cases: measles outbreak in the Provence-Alpes-Côte d'Azur region, France, January to November 2010-substantial underreporting of cases. *Euro Surveill* 2010;**15**(50).
2. Botelho-Nevers E, Cassir N, Minodier P, Laporte R, Gautret P, Badiaga S, et al. Measles among healthcare workers: a potential for nosocomial outbreaks. *Euro Surveill* 2011;**16**(2).
3. Wagner KS, White JM, Lucenko I, Mercer D, Crowcroft NS, Neal S, et alDiphtheria Surveillance Network. Diphtheria in the postepidemic period, Europe, 2000–2009. *Emerg Infect Dis* 2012;**18**(2):217–25.
4. Bonmarin I, Guiso N, Le Flèche-Matéos A, Patey O, Patrick AD, Levy-Bruhl D. Diphtheria: a zoonotic disease in France? *Vaccine* 2009;**27**(31):4196–200.
5. Rousseau C, Belchior E, Broche B, Badell E, Guiso N, Laharie I, et al. Diphtheria in the south of France, March 2011. *Euro Surveill* 2011;**16**(19).
6. Geddes JR, Fazel S. Extreme health inequalities: mortality in homeless people. *Lancet* 2011;**377**(9784):2156–7.
7. Levy BD, O'Connell JJ. Health care for homeless persons. *N Engl J Med* 2004;**350**(23):2329–32.
8. Launay O, Toneatti C, Bernède C, Njamkepo E, Petitprez K, Leblond A, et al. Antibodies to tetanus, diphtheria and pertussis among healthy adults vaccinated according to the French vaccination recommendations. *Hum Vaccin* 2009;**5**(5):341–6.
9. Senouci H, Lounici M, Rahal K. Antidiphtheria immunity of the Algerian population: a seroepidemiological study. *Med Mal Infect* 2004;**34**(7):316–20. French.
10. Rouahi N, Biognach H, Benchellal M, Zouhdi M. Attentiveness face to tetanus and diphtheria immunity for students between 2004 and 2005 in Morocco. *Immuno-analyse & Biologie Spécialisée* February 2009;**24**(1):37–41.

Samir Benkouiten
Sékéné Badiaga
Claude Nappez
Aix Marseille Université, URMITE, UMR CNRS 7278, IRD 198, Inserm 1095, 13005 Marseille, France

Rémi Charrel
UMR190 Emergence des Pathologies Virales (Aix Marseille Université – IRD – EHESP), 13005 Marseille, France

Didier Raoult
Philippe Brouqui*
Aix Marseille Université, URMITE, UMR CNRS 7278, IRD 198, Inserm 1095, 13005 Marseille, France
E-mail addresses: philippe.brouqui@univ-amu.fr, philippe.brouqui@ap-hm.fr (P. Brouqui)

*Corresponding author. Tel.: +33 491 32 43 75; fax: +33 491 38 77 72.

Accepted 20 October 2012

http://dx.doi.org/10.1016/j.jinf.2012.10.023

Seroepidemiology of Saffold cardiovirus (SAFV) genotype 3 in Japan

Dear Editor,

A new virus, Saffold cardiovirus (SAFV) belonging to genus Cardiovirus of family Picornaviridae has been identified and characterized, but its pathogenesis is not yet fully understood.[1,2] SAFV type 3 (SAFV3) is thought to be the major genotype and is relatively frequently detected in patients with acute gastroenteritis and respiratory illness.[3–5] In attempts to elucidate the pathogenesis, we conducted a seroepidemiological study of SAFV3 in Japanese people.

A total of 114 serum samples from subjects aged 0–66 years were collected in Gunma prefecture, Japan, in 2010. Subjects aged ≤5 years showed no evidence of infectious disease with minor congenital cardiac defect or inguinal

Table 1 Seropositivity of SAFV3 in the present subjects.

Age (year)	Positive rate (positive/total)	Total	GMT
0–1	76.9 (10/13)	13	30.7
2–4	84.6 (11/13)	13	36.3
5–9	100 (14/14)	14	72.9
10–19	100 (15/15)	15	80.6
20–	100 (59/59)	59	79.1
Total	95.6 (109/114)	114	66.1

GMT, geometric mean titers.

hernia. Other subjects were healthy volunteers. All samples were collected after obtaining informed consent from subjects or their parents/guardians. We measured neutralization antibodies in the serum using a representative SAFV3 isolate from a child with upper respiratory infection.[6] The neutralization antibody titer was measured using MRC-5 cells and results greater than or equal to 1:4 were considered positive. Statistical analysis was performed by the χ^2 test using SPSS software (SPSS for Windows, version 10.0). A p value of <0.05 was regarded as statistically significant.

Antibodies against SAFV3 were found in 95.6% of samples (Table 1). Notably, 100% of subjects aged ≥5 years had SAFV3 specific antibodies. The geometric mean titers (GMT) of neutralization antibodies to SAFV in subjects aged 0–1, 2–4, 5–10, 11–19, and ≥20 years were 30.7, 36.3, 72.9, 80.6, and 79.1, respectively. Subjects aged ≥5 years had significantly higher GMT of neutralizing antibodies to SAFV than those ≤4 years ($p < 0.05$). These results suggest that SAFV3 is a common agent in our population. Indeed, more than 90% of individuals of 5 years of age showed evidence of exposure to SAFV3. A previous report suggested that SAFV3 is a highly common virus causing infection in early childhood in Europe (Finland and the Netherlands), Africa (Cameroon and Mali), and Asia (Indonesia).[7] In Japan, on the other hand, Hosomi et al. showed that seropositivity against SAFV3 was relatively low in subjects aged ≤5 years and the elderly.[8] This discrepancy in findings may be due to differences in the assay (cut-off value), regional differences, and differences in the SAFV3 strains used in the neutralization antibody assay.[8]

To date, at least 8 genotypes of SAFV have been confirmed, but the pathogenicity and antigenicity of these viruses remain obscure.[2] However, cases of severe SAFV infection have been reported.[9] Thus, additional detailed epidemiological studies are needed to ascertain both the characteristics of each genotype of SAFV and the relationships between genotypes.

Competing interests

The authors declare that they have no competing interests. The authors alone are responsible for the content and writing of the paper.

Acknowledgments

This work was supported by a Grant-in-Aid from the Japan Society for Promotion of Science and for Research on Emerging and Re-emerging Infectious Diseases from the Ministry of Health, Labor, and Welfare, Japan.

References

1. Jones MS, Lukashov VV, Ganac RD, Schnurr DP. Discovery of a novel human picornavirus in a stool sample from a pediatric patient presenting with fever of unknown origin. *J.Clin.Microbiol.* 2007;**45**:2144–50.
2. Himeda T, Ohara Y. Saffold virus, a novel human Cardiovirus with unknown pathogenicity. *J Virol* 2012;**86**:1292–6.
3. Chiu CY, Greninger AL, Kanada K, Kwok T, Fischer KF, Runckel C, et al. Identification of cardioviruses related to Theiler's murine encephalomyelitis virus in human infections. *Proc Natl Acad Sci USA* 2008;**105**:14124–9.
4. Tsukagoshi H, Mizuta K, Abiko C, Itagaki T, Yoshizumi M, Kobayashi M, et al. The impact of Saffold cardiovirus in patients with acute respiratory infections in Yamagata, Japan. *Scand J Infect Dis* 2011;**243**:669–71.
5. Ren L, Gonzalez R, Xiao Y, Xu X, Chen L, Vernet G, et al. Saffold cardiovirus in children with acute gastroenteritis, Beijing, China. *Emerg Infect Dis* 2009;**15**:1509–11.
6. Tsukagoshi H, Masuda Y, Mizutani T, Mizuta K, Saitoh M, Morita Y, et al. Sequencing and phylogenetic analyses of Saffold cardiovirus (SAFV) genotype 3 isolates from children with upper respiratory infection in Gunma, Japan. *Jpn J Infect Dis* 2010;**63**: 378–80.
7. Zoll J, Erkens Hulshof S, Lanke K, Verduyn Lunel F, Melchers WJ, Schoondermark-van de Ven E, et al. Saffold virus, a human Theiler's-like cardiovirus, is ubiquitous and causes infection early in life. *PLoS Pathog* 2009;**5**:e1000416.
8. Hosomi T, Nabeshima T, Taniwaki T, Matsumoto K, Fujito A, Geshi I, et al.. Prevalence of neutralizing antibody against Saffold virus genotypes 2 and 3 in Kochi, Japan, abstr VI-PO47–9. Inter union of microbiological societies 2011congress, 2011.
9. Nielsen AC, Böttiger B, Banner J, Hoffmann T, Nielsen LP. Serious invasive Saffold virus infections in children, 2009. *Emerg Infect Dis* 2012;**18**:7–12.

Miho Kobayashi
Hiroyuki Tsukagoshi
Taisei Ishioka
Gunma Prefectural Institute of Public Health and Environmental Sciences, 378 Kamioki-machi, Maebashi-shi, Gunma 371-0052, Japan

Katsumi Mizuta
Yamagata Prefectural Institute of Public Health, 1-6-6 Toka-machi, Yamagata-shi, Yamagata 990-0031, Japan

Masahiro Noda
Infectious Diseases Surveillance Center, National Institute of Infectious Diseases, 4-7-1 Gakuen, Musashimurayama-shi, Tokyo 208-0011, Japan

Yukio Morita
Department of Nutritional Science, Tokyo Kasei University, 1-18-1 Kaga, Itabashi-ku, Tokyo 173-8602, Japan

Akihide Ryo
Department of Molecular Biodefence Research, Yokohama City University Graduate School of Medicine, 3-9 Fukuura, Kanazawa-ku, Yokohama-shi, Kanagawa 236-0004, Japan